T.C.
DOKUZ EYLUL UNIVERSITY
IZMIR INTERNATIONAL
BIOMEDICINE AND GENOME
INSTITUTE

A PORTABLE ELECTROCHEMICAL BIOSENSOR FOR HIGHLY SENSITIVE AUTOMATED-QUANTITATIVE ANALYSIS OF ANALYTES

FATMA KURUL

BIOMEDICINE AND HEALTH TECHNOLOGIES

MASTER OF SCIENCE THESIS

IZMIR-2024

THESIS ID: DEU.HSI.MSc/2020850033

T.C.
DOKUZ EYLUL UNIVERSITY
IZMIR INTERNATIONAL
BIOMEDICINE AND GENOME
INSTITUTE

A PORTABLE ELECTROCHEMICAL BIOSENSOR FOR HIGHLY SENSITIVE AUTOMATED-QUANTITATIVE ANALYSIS OF ANALYTES

BIOMEDICINE AND HEALTH TECHNOLOGIES

MASTER OF SCIENCE THESIS

FATMA KURUL

Supervisor: Assoc. Prof. Dr. Serhat TOZBURUN

Co-Supervisor: Dr. Arif Engin ÇETİN

THESIS ID: DEU.IBG.MSc/2020850033

Dokuz Eylül University İzmir International Biomedicine and Genome Institute Department of Biomedicine and Health Technologies, Biomedicine and Health Technologies graduate program Master of Science student Fatma KURUL has successfully completed her Master of Science thesis titled '**A Portable Electrochemical Biosensor for Highly Sensitive Automated-Quantitative Analysis of Analytes**' on the date of 05.02.2024.

Assoc. Prof. Dr. Serhat TOZBURUN
Dokuz Eylül University
CHAIR

MEMBER

Prof. Dr. Seda Nur TOPKAYA ÇETİN
Izmir Katip Celebi University

MEMBER

Assoc. Prof. Muhammed ÜÇÜNCÜ
Izmir Katip Celebi University

SUBSTITUTE MEMBER

Prof. Dr. Sinem Ezgi TURUNÇ ÖZOĞLU
Izmir Katip Celebi University

SUBSTITUTE MEMBER

Assos. Prof. Hüseyin İSTANBULLU
Izmir Katip Celebi University

Dokuz Eylül Üniversitesi İzmir Uluslararası Biyotıp ve Genom Enstitüsü Biyotıp ve Sağlık Teknolojileri Anabilim Dalı, Biyotıp ve Sağlık Teknolojileri Yüksek Lisans programı öğrencisi Fatma KURUL **'Analitlerin Yüksek Hassasiyette Otomatik Nicel Analizine Yönelik Portatif Elektrokimyasal Biyosensör'** konulu Yüksek Lisans tezini 05.02.2024 tarihinde başarılı olarak tamamlamıştır.

Doç. Dr. Serhat TOZBURUN

Dokuz Eylül Üniversitesi

BAŞKAN

ÜYE

Prof. Dr. Seda Nur TOPKAYA ÇETİN

İzmir Katip Çelebi Üniversitesi

ÜYE

Doç. Dr. Muhammed ÜÇÜNCÜ

İzmir Katip Çelebi Üniversitesi

YEDEK ÜYE

Prof. Dr. Sinem Ezgi TURUNÇ ÖZOĞLU

İzmir Katip Çelebi Üniversitesi

YEDEK ÜYE

Dr. Öğr. Üyesi Hüseyin İSTANBULLU

İzmir Katip Çelebi Üniversitesi

TABLE OF CONTENTS

LIST OF TABLES ..... **IV**

LIST OF FIGURES ..... **V**

LIST OF ABBREVIATIONS ..... **VIII**

ACKNOWLEDGEMENTS ..... **XI**

ABSTRACT **2**

ÖZET **3**

1. INTRODUCTION AND AIM **4**

1.1. Statement and Importance of the Problem **4**

1.2. Aim of the Study **4**

1.3. Hypothesis of the Study **5**

2. GENERAL INFORMATION **6**

2.1. Voltammetry **6**

2.2. Types of Electrodes Used in Voltammetry **7**

2.2.1. Working Electrode **7**

2.2.2. Reference Electrode **8**

2.2.3. Counter Electrode **9**

2.2.4. Screen-printed Electrodes **9**

2.3. Biosensors **11**

2.4. Development of DNA-Electrochemical Biosensors **14**

2.5. Immobilization Techniques in Biosensors **15**

2.5.1. Physical Adsorption **15**

2.5.2. Covalent Binding **15**

2.5.3. Cross Linking **16**

2.5.4. Entrapment **16**

2.5.5. Encapsulation **16**

2.6. Deoxyribonucleic Acid (DNA) Structure **16**

2.7. Types of DNA-Drug Interaction **17**

2.8. Drug Candidate Molecules **18**

3. MATERIALS AND METHODS **19**

3.1. Type of the Study **19**

3.2. Time and Location of the Study **19**

3.3. The Universe and Sample of Research **19**

3.4. Working Materials **20**

3.4.1. Apparatus and Instruments **20**

3.4.2. Chemicals **20**

3.4.3. Synthesis of Drug Candidate Molecules **20**

3.5. Optimization Study of Drug Candidate Molecules using a Three Electrode System **21**

3.5.1. Optimization of pH ***23***

3.5.2. Optimization of Drug Concentration ***23***

3.5.3. Scan Rate Study ***23***

3.5.4. Stability Study ***23***

3.5.5. Interaction Study with dsDNA ***24***

3.6. Comparative Studies using Screen-printed Electrode-based Electrochemical Biosensor **25**

3.6.1. Development of Electrochemical Biosensor Platform ***26***

3.6.2. Graphical User Interface (GUI) ***28***

3.6.3. Testing Procedure ***30***

3.7. Data Collection Tools **31**

3.8. Research Plan **32**

3.9. Data Evaluation **32**

3.10. Limits of Study **32**

4. RESULTS AND DISCUSSIONS **33**

4.1. Effect of pH **33**

4.2. Effect of Concentration **36**

4.3. Effect of Scan Rate **37**

4.4. Stability Results **39**

4.5. Interaction Results **40**

4.6. Results of Screen-Printed Electrode (SPE) Experiments **42**

5. DISCUSSIONS **44**

6. CONCLUSION AND FUTURE DIRECTIONS **46**

7. REFERENCES **48**

8. APPENDIX **58**

8.1. NMR Spectra of Drug Candidate Molecules **58**

8.2. Research Ethics Committee Approvals **64**

8.3. Curriculum Vitae **65**

LIST OF TABLES

Table 1. Overview of current research on screen-printed electrode-based studies..... 10

Table 2. The ingredients of the buffer solutions for different pH values..... 23

Table 3. Technical specifications of PalmSens4..... 31

LIST OF FIGURES

Figure 1. Excitation signals for various voltammetric methods, including CV (A), DPV (B), and SWV (C), and their response graphs of potential against current (T; waveform period, S1 and S2; two current, ΔE potential increment) [13]. 7

Figure 2. Applications of biosensors in various fields, including drug development, disease detection, pathogen discovery, and environmental monitoring. It was created with BioRender.com. 12

Figure 3. General schematic of a biosensor consisting of analyte, bioreceptor, and transducer [53]. It was created with BioRender.com. 12

Figure 4. General schematic of the DNA-based biosensor [81]. 14

Figure 5. The DNA structure consisting of nucleotides (A, Adenine; T, Thymine; G, Guanine; and C, Cytosine)[91]. 17

Figure 6. Chemical structure of drug candidate molecules: D_1-TP, D_2-TP and D_3-TP. 21

Figure 7. Activation process of PEGs: PEGs were cut into 3 mm lengths and activated by applying +1.4 V for 30 seconds in ACB at pH 4.8. 22

Figure 8. The experimental setup consisted of a PalmSens operating as a potentiostat, a three-electrode system, and a graphical user interface. 22

Figure 9. Investigation of the interaction between D_1-TP, D_2-TP, and D_3-TP with dsDNA, respectively. 25

Figure 10. The general scheme of this study includes drug synthesis, optimization studies with a three-electrode system, and DNA-drug interaction tests with SPE. 26

Figure 11. The bottom and top resin-based molds and PDMS layers. 27

Figure 12. In the photograph of the sample apparatus (A), SPEs were sandwiched between PDMS layers, which were then inserted between two acrylic caps (B). 28

Figure 13. Graphical user interface. 29

Figure 14. The general figure of electrochemical biosensor. 30

Figure 15. Schematic presentation for electrochemical detection of Ds-TP interaction with dsDNA using screen-printed electrodes. 31

Figure 16. The effect of pH on peak currents of Ds-TP. The bar graph depicts drug candidates with a pH of 3.8–7.4. Error bars represent standard deviation (ns, not significant). 33

Figure 17. The DPV voltammogram of D_1-TP (ACB, pH 3.8). D_1-TP displayed oxidation peak potentials at 1.04 V and 1.14 V. (*The DPV voltammogram represents the result of a single measurement.) 34

Figure 18. DPV voltammograms of D_2-TP (ACB, pH 3.8). D_2-TP showed two peak potentials at 0.79 and 1.10 V. (*The DPV voltammogram represents the result of a single measurement.) 34

Figure 19. DPV voltammograms of D_3-TP (ACB, pH 5.6). D_3-TP exhibited two peak potentials at 0.76 V and 1.05 V. (*The DPV voltammogram represents the result of a single measurement.) 35

Figure 20. DPV measurements were carried out (scan rate, 100 mV/s) using concentrations ranging from 5 to 20 µg/mL of D_1-TP immobilized on PGE (A). The calibration curve demonstrates the relationship between the first oxidation signal of D_1-TP and its concentration (B)..... 36

Figure 21. DPV measurements were performed (scan rate, 100 mV/s) using varying concentrations ranging from 5 to 20 µg/mL of D_2-TP immobilized on PGE (A), and the calibration curve was obtained using the first oxidation current of D_2-TP (B)..... 36

Figure 22. DPV measurements were carried out at (scan rate, 100 mV/s) using varying concentrations of D_3-TP from 2.5 µg/mL to 20 µg/mL (A), and the calibration curve was obtained using the first oxidation current of D_3-TP (B)..... 37

Figure 23. The effect of the scan rate on the peak current was investigated through CV measurements conducted at scan rates ranging from 25 to 150 mV/s. 38

Figure 24. Calibration plot of log scan rate Vs log current of drug candidates. 38

Figure 25. Bar graph expressing the stability of D_1-TP, D_2-TP and D_3-TP investigated under storage conditions by monitoring DPV technique. DPV voltammograms of drug candidates were recorded after preparation, 5 days, 7 days, 14 days and 30 days..... 39

Figure 26. The interaction of D_1-TP with dsDNA. The DPVs were recorded on bare PGE (red), PGE coated with D_1-TP (turquoise), PGE coated with dsDNA (purple), and PGE coated with dsDNA+D_1-TP (orange)..... 40

Figure 27. The interaction of D_2-TP with dsDNA. The DPVs were recorded on bare PGE (red), PGE coated with D_2-TP (turquoise), PGE coated with dsDNA (purple), and PGE coated with DNA+D_2-TP (orange). 41

Figure 28. Interaction of D_3-TP–dsDNA. The DPVs were recorded on bare PGE (red), PGE coated with D_3-TP (turquoise), PGE coated with dsDNA (purple), and PGE coated with DNA+D_3-TP (orange). 42

Figure 29. Interaction of D_1-TP–dsDNA. DPV measurements were conducted to analyze the interaction of D_1-TP with dsDNA-modified SPE. DPVs were recorded on different electrodes: bare SPE (red), SPE coated with D_1-TP (turquoise), SPE coated with dsDNA (purple), and SPE coated with DNA+D_1-TP (orange)..... 42

Figure 30. Interaction of D_2-TP–dsDNA. DPV measurements were conducted to analyze the interaction of D_2-TP with dsDNA-modified SPE. DPVs were recorded on different electrodes: bare SPE (red), SPE coated with D_2-TP (turquoise), SPE coated with dsDNA (purple), and SPE coated with DNA+D_2-TP (orange)..... 43

Figure 31. Interaction of D_3-TP–dsDNA. DPV measurements were conducted to analyze the interaction of D_3-TP with dsDNA-modified SPE. DPVs were recorded on different electrodes: bare SPE (red), SPE coated with D_3-TP (turquoise), SPE coated with dsDNA (purple), and SPE coated with DNA+ D_3-TP (orange)..... 44

LIST OF ABBREVIATIONS

° : Degree

°C : Celsius Degree

µ : Micro - (10^{-6})

µg : Microgram

µL : Microliter

A : Adenine

ACB : Acetate Buffer

C : Cytosine

CE : Counter Electrode

CH_3COOH: Acetic Acid

CPE : Carbon Paste Electrode

CV : Cyclic Voltammetry

Cs_2CO_3 : Cesium Carbonate

DI water : Deionized Water

DMF : Dimethylformamide

DNA : Deoxyribonucleic Acid

DPV : Differential Pulse Voltammetry

dsDNA : Double Stranded Deoxyribonucleic Acid

G : Guanine

GCE : Glassy Carbon Electrodes

GUI : Graphical User Interface

H_3BO_3 : Boric Acid

KCl : Potassium chloride

KH_2PO_4 : Potassium dihydrogen phosphate

K_2HPO_4 : Dipotassium phosphate

mL : Milliliter

NaCl : Sodium chloride

NaOH : Sodium hydroxide

LOD : Limit of Detection

LOQ : Limit of Quantification

pH : Power of Hydrogen

PBS : Phosphate Buffer

PDMS : Polydimethylsiloxane

PGE : Pencil Grafite Electrode

RE : Reference Electrode

s : Second

SCE : Saturated Calomel Electrode

SPE : Screen Printed Electrode

SWV : Square Wave Voltammetry

T : Thymine

TE : Tris-EDTA

UPW : UltraPure Water

V : Potential

WE : Working Electrode

DEDICATION

This thesis is dedicated to my family, who love me, taught me perseverance, and strengthened me. I have reached this point with your help, and I will go even further.

Fatma Kurul

Izmir, 2024

ACKNOWLEDGEMENTS

I am deeply grateful to several individuals who have played a crucial role in completing my thesis. My sincerest thanks go to my supervisor, *Assoc. Prof. Dr. Serhat Tozburun* for his exceptional supervision and guidance throughout the thesis project. I want to thank my co-supervisor, *Dr. Arif Engin Çetin.* He opened the doors of his laboratory to me. Special thanks to *Prof. Dr. Seda Nur Topkaya Çetin* for her motivating guidance. I would like to thank *Ass. Prof. Hüseyin İstanbullu* for the synthesis of the drug candidate molecules used in my thesis.

I would like to express my gratitude to *Mehmet Kocagöz* for being there on my side and making me happy throughout this journey. I want to thank my family for their patience, support and encouragement.

I want to express my sincere gratitude to *Prof. Dr. Berna Özkale Edelmann* for generously welcoming me into her laboratory during my Erasmus journey. I would like to express special thanks to *Philipp Harder* for his mentorship during my Erasmus experience. I am sincerely grateful to *Dr. Sena Yaman* for her invaluable support and guidance during my initial exploration of microfluidic systems.

I want to thank all my lab friends, *Bilge Can, Meryem Beyza Avcı, and Damla Aydoğan,* for their valuable friendship. Special thanks go to my IBG friends *Tuğba Topbaş, Burak Kahveci, Elçin Çağatay, Yonca Güngör* and *İnci Yaprak.* Your support has turned my academic journey into an unforgettable adventure. I am happy to have found lifelong friends. I would like to thank *Fatma Nur Bedeloğlu, Şeyma Göner, Kutay Bulut, Feryal Sunar, Eda Karataş, Hezzal Küçükselbes, Çigdem Yener, Sinem Karatekin, Büşra Nur Özkaya, Şeyma Gümüş, Meryem Akkurt and Bekir Göktaş* for their never-ending support.

I want to thank *The Scientific and Technological Research Council of Turkey (TUBİTAK)* for their support through the *BİDEB/2210-D Domestic Industry Graduate Scholarship Program.*

Thank you all again.

Fatma KURUL

A PORTABLE ELECTROCHEMICAL BIOSENSOR FOR HIGHLY SENSITIVE AUTOMATED-QUANTITATIVE ANALYSIS OF ANALYTES

Fatma Kurul, Izmir International Biomedicine and Genome Institute, Dokuz Eylul University

ABSTRACT

DNA is a critical molecule that contains our genetic information and is a crucial pharmacological target for drug candidate molecules. Investigating the effect of drug candidate molecules on the DNA is essential for developing new drugs. Electrochemical analysis techniques are widely used in examining the interactions between DNA and drug molecules. In electrochemical analyses, a three-electrode system consisting of a reference electrode (RE), a working electrode (WE), and a counter electrode (CE) is utilized. With the rapid development of screen printing technology, screen-printed electrodes (SPE) containing RE, WE and CE electrodes have gained considerable attention.

In this thesis, three novel new triazolopyrimidinone derivatives, D_1-TP, D_2-TP, and D_3-TP, were synthesized as drug candidates. The electrochemical behaviours of these drug candidates were explored for the first time using electrochemical techniques. Subsequently, the effects of potential drug candidates on dsDNA (double-stranded DNA) were investigated.

The obtained data using the three-electrode system indicates that drug candidates can be analyzed in a biosensor system. In this context, a portable and user-friendly electrochemical biosensor system based on SPE has been developed. The biosensor system includes a simple and user-friendly interface implemented using the C# programming language. This system has the potential to be used in various fields, such as environmental monitoring, food safety, and biomedicine.

Key Words: Triazolopyrimidinone, candidate drug molecule, DNA-drug interaction, electrochemical biosensor, screen-printed electrode.

ANALİTLERİN YÜKSEK HASSASİYETTE OTOMATİK NİCEL ANALİZİNE YÖNELİK PORTATİF ELEKTROKİMYASAL BİYOSENSÖR

Fatma Kurul, İzmir Uluslararası Biyotıp ve Genom Enstitüsü, Dokuz Eylül Üniversitesi

ÖZET

DNA, genetik bilgilerimizi içeren kritik bir moleküldür ve ilaç aday molekülleri için çok önemli bir farmakolojik hedeftir. İlaç aday moleküllerinin DNA molekülü üzerindeki etkilerinin incelenmesi yeni ilaçların geliştirilmesi açısından önemlidir. Elektrokimyasal analiz teknikleri, DNA ve ilaç molekülleri arasındaki etkileşimlerin araştırılmasında yaygın olarak kullanılmaktadır. Elektrokimyasal analizlerde, bir referans elektrodu (Reference Electrode; RE), bir çalışma elektrodu (Working Electrode; WE) ve bir karşı elektrot (Counter Electrode; CE) içeren üçlü elektrot sistemi kullanılmaktadır. Serigrafi baskı teknolojisinin hızla gelişmesiyle birlikte referans, çalışma ve karşıt elektrotları içeren Perde Baskılı Elektrotlar (Screen Printed Electrode; SPE) büyük ilgi görmüştür.

Bu tez çalışmasında, üç yeni triazolopirimidinon türevi, D_1-TP, D_2-TP ve D_3-TP, ilaç aday molekülleri olarak sentezlendi. İlaç aday moleküllerinin elektrokimyasal özellikleri elektrokimyasal teknikler kullanılarak ilk kez incelendi. Daha sonra ilaç aday moleküllerinin çift sarmallı DNA (dsDNA) üzerindeki etkileri araştırıldı.

Üçlü elektrot sistemi kullanılarak elde edilen veriler, ilaç adaylarının bir biyosensör sisteminde analiz edilebileceğini göstermektedir. Bu bağlamda SPE tabanlı taşınabilir ve kullanıcı dostu bir elektrokimyasal biyosensör sistemi geliştirilmiştir. Biyosensör sistemi, C# programlama dili kullanılarak geliştirilen basit ve kullanıcı dostu bir arayüz içermektedir. Bu sistem çevre izleme, gıda güvenliği, biyotıp gibi çeşitli alanlarda kullanım potansiyeline sahiptir.

Anahtar Kelimeler: Triazolopirimidinon, ilaç aday molekülü, DNA-ilaç etkileşimi, elektrokimyasal biyosensör, perde baskılı elektrot.

1. INTRODUCTION AND AIM

1.1. Statement and Importance of the Problem

DNA is a critical molecule that contains our genetic information [1] and is essential to many vital processes, including transcription, protein synthesis, and replication [2]. DNA controls cell functions by regulating the expression of genes through transcription and the production of proteins through translation or by disrupting the process of replication, which is crucial for cell growth and division [3]. DNA is also a popular drug target, considering its pivotal role in various disease mechanisms. DNA analysis is essential to the development of novel targeted drugs. Understanding how drugs interact with DNA is crucial for developing new targeted drugs and can offer valuable insights into how these drugs work to produce therapeutic effects [4].

Recently, triazolopyrimidinone compounds have gained significant attention across various fields, exhibiting multiple activities such as antiviral, anticancer, antitumoral and antioxidant [5]. In this study, compounds derived from triazolopyrimidinone were synthesized and referred to as D_1-TP, D_2-TP, and D_3-TP. The exploration of the electrochemical behaviours of novel triazolopyrimidinone derivatives is essential for understanding their pharmaceutical effects. Additionally, investigating their interactions with DNA is crucial in assessing their potential as new drug candidates. This is the first report to investigate the electrochemical characteristics of these therapeutic candidates and their interaction mechanism with dsDNA.

Furthermore, following optimization studies, an electrochemical biosensor-integrated SPE will be developed for comprehensive testing, explicitly focusing on examining the interactions between these novel triazolopyrimidinone derivatives and dsDNA. Electrochemical biosensors are essential tools in drug development. They are used to screen new antitumor drugs, measure DNA-drug interactions for pharmacokinetic studies, and contribute to the design of novel drugs. Additionally, these biosensors are valuable for developing straightforward analytical devices for point-of-care testing.

1.2. Aim of the Study

This study will investigate the electrochemical behaviours of novel triazolopyrimidinone derivatives. One of the compounds synthesized in this study, D_1-TP, will be introduced to the literature. D_2-TP and D_3-TP compounds have been previously studied; this

study provides their complete spectral characterization for the first time in the literature (Patent No; WO 2010/056630 A2).

The main aim of this study is to examine the electrochemical behaviours of these triazolopyrimidinone derivatives using pencil graphite electrodes. The effect of various experimental factors, pH, scan rate, and concentration will be examined. The stability of novel triazolopyrimidinone derivatives will be evaluated on specific days.

The second aim is to analyze their interactions with dsDNA to understand the mechanisms behind their pharmacological effects. The interactions of drug-candidate molecules with DNA will be investigated by monitoring oxidation signals of A and G bases.

The final aim of this thesis is to produce a screen-printed electrode-integrated electrochemical biosensor system that is important for detecting pharmaceutical compounds. The biosensor system will comprise a user interface, a sample apparatus, and a transducer system. The sample apparatus will include three separate sample chambers, allowing direct access of the sample placed on the SPE to the entire working electrodes through PDMS channels, thereby minimizing sample usage. While the potentiostat comes with its Software, a Graphical User Interface (GUI) will be developed to generate graphs without the need for Excel to evaluate DNA-drug interaction analysis results. The potentiostat will be utilised as the transducer system, providing the fundamental control and measurement mechanism for the biosensor system.

1.3. Hypothesis of the Study

The electrochemical behaviour of triazolopyrimidinone derivatives will be analyzed using a reliable and reproducible method using a screen-printed electrode-integrated electrochemical biosensor system. This biosensor system will help us understand the interaction mechanism between triazolopyrimidinone derivatives and dsDNA based on guanine signals. In addition, a user-friendly interface created using the C# programming language will integrated into this biosensor system. Guanine, a fundamental DNA building block, is crucial for carrying genetic information. When it interacts with a drug molecule, this interaction often results in changes to guanine bases. These changes can provide insights into how the drug interacts with DNA and its potential biological effects.

2. GENERAL INFORMATION

2.1. Voltammetry

Voltammetry is a family of electroanalytical techniques that is a widely used tool for studying electrochemical reactions nowadays. It depends on the voltage-current responses observed in an electrochemical cell that consists of three electrodes: WE, CE, and RE. This method obtains data on an analyte by monitoring the voltage-current responses.

This technique involves acquiring information about an analyte by measuring the current as the potential changes. The outcomes of a voltammetric experiment are presented in the form of a voltammogram, a graphical representation depicting the current plotted against the potential [6], [7]. Various potential excitation signals are applied to the WE during the electrochemical reaction. The resulting current responses vary depending on the type of excitation signal employed. **Fig. 1** shows the excitation signals of cyclic voltammetry (CV), differential pulse voltammetry (DPV), and square wave voltammetry (SWV).

In CV, a triangular waveform is applied on the working electrode to scan the potential, allowing the observation of the resulting current. In alternating voltammetry applications, the potential undergoes oscillations between two values, characterized by a linear increase towards a maximum and a subsequent linear decrease back to the original value. Simultaneously, when the applied potential approaches equilibrium, the response current increases. The attainment of equilibrium between charge transfer and diffusion actions results in the emergence of a discernible oxidation peak [8]–[10]. Examining the peaks in the voltammogram provides essential insights into the reaction mechanism, revealing details about redox potential, reaction reversibility, and analyte concentration [11], [12].

In DPV, a potential pulse is superimposed on a linearly changing potential (a step potential). The resulting current response is measured at a specific time after the pulse. The numerical difference between both samples is then determined to obtain a relatively Faradaic current [14], [15]. Due to its high sensitivity, DPV is the ideal technique for detecting traces of inorganic and biological compounds [16].

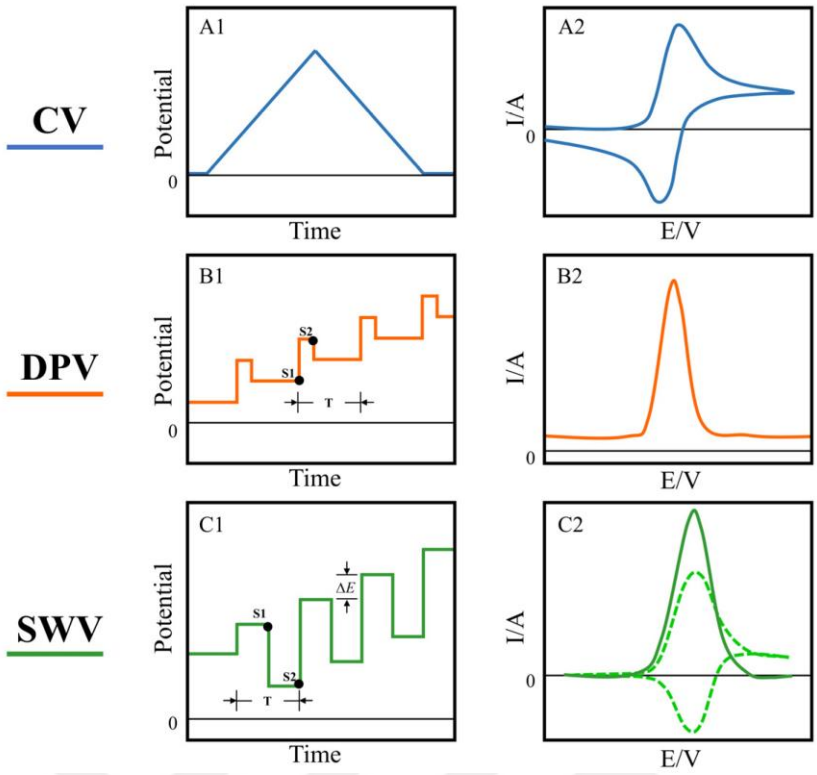


Figure 1. Excitation signals for various voltammetric methods, including CV (A), DPV (B), and SWV (C), and their response graphs of potential against current (T; waveform period, S1 and S2; two current, ΔE potential increment) [13].

SWV is an advanced electrochemical technique for sensitively analysing electroactive species in many fields, including chemistry, biology, and environmental science [17], [18]. SWV is characterized by its square-wave potential waveform superimposed onto a staircase-like voltage ramp. This unique waveform allows for the separation of faradaic current from capacitive current, reducing background noise and enhancing the sensitivity of the analysis. Due to its remarkable signal-to-noise ratio, SWV is particularly effective in detecting and quantifying trace amounts of analytes in complex samples. It offers advantages such as rapid data acquisition, low detection limits, and the ability to perform measurements at relatively high scan rates.

2.2. Types of Electrodes Used in Voltammetry

2.2.1. Working Electrode

The working electrode (WE) ensures that the desired electrochemical reaction can be carried out effectively and efficiently [8]. The WE is a transducer that responds to the

electrochemical reaction [19]. The primary purpose of the working electrode is facilating efficient electron transfer to the substrate while having a high activation energy for electron transfer in the primary competing reaction. Types of carbon electrodes commonly used as working electrodes include carbon paste electrodes (CPE)[20], glassy carbon electrodes (GCE)[21] and pencil graphite electrodes (PGE) [22], [23]. Among them, pencil graphite electrodes are commonly utilized primarily due to their cost-effectiveness and convenient disposability. With an adaptable working surface area, they facilitate rapid analyses and enable the determination of low concentrations in the target solution [24]. They are also commonly preferred tools in pharmaceutical studies.

Antherjanam and co-workers produced a low-cost sensor to analyze the hydroxylamine (HA) and hydrazine (HY) using modified PGEs. HY and HA are hazardous environmental pollutants and highly toxic to organisms. Tap and river water samples containing HA and HY were used to test this electrochemical biosensor. It revealed the most significant concentration range for the simultaneous study of HA and HY that has been reported so far [25].

Šafranko et al. analyzed the oxidation mechanism and electrochemical behaviour of hesperidin using a disposable PGE for the first time. They optimized some experimental (pH, concentration) parameters on hesperidin using the DPV technique. The LOD was found to be 2×10^{-7} mol dm^{-3} [26].

Mirmomtaz and co-workers introduced a precision electrochemical technique for analysing dsDNA interaction with amiloride using PGE. They also used ds-DNA-modified PGE to determine amiloride levels in actual samples. Using the suggested technique, the effect of amiloride on dsDNA can be easily identified and rapidly detected in actual samples [27].

2.2.2. Reference Electrode

The reference electrode (RE) is critical for measuring and controlling potential [28]. It is designed to exhibit reversible Nernstian behaviour, maintaining a constant and well-known electrode potential throughout the reactions. Two commonly employed reference electrodes are the Ag/AgCl and the calomel electrode [29].

a) Ag/AgCl Electrode

Ag/AgCl reference electrodes are a type of aqueous electrode with a potential reference

to the hydrogen standard electrode. The following reaction determines the potential of the Ag/AgCl electrode [30]:

$$AgCl\ (s) + e^- \rightleftarrows Ag\ (s) + Cl^- \quad \textbf{(1)}$$

The potential of electrodes is stable and reversible, and it is widely used in electrochemical experiments due to its reliability and reproducibility. This electrode remains unaffected by variations in temperature and pressure, demonstrating compatibility with a different type of solutions.

b) Calomel Electrode

The saturated calomel electrode (SCE) has several dimensions and shapes. It is typically in the form of a calomel-saturated electrode, which is produced by the reaction between mercury (Hg) and mercury chloride (Hg_2Cl_2). The aqueous phase is typically made with saturated potassium chloride solutions. The potential of the SCE is determined by the following simple reaction [31]:

$$Hg_2Cl_2\ (s) + 2e^- \rightleftarrows 2Hg\ (l) + 2Cl^- \quad \textbf{(2)}$$

This electrode is widely used in electrochemical experiments because of its stability and reproducibility.

2.2.3. Counter Electrode

The counter electrode (CE) is usually constructed of platinum wire but can be made from graphite or gold [32]. The counter electrode typically consists of an inert material with a large surface area. It is used for the flow of electrons. During voltammetric analysis, the reactions at the electrode surfaces are fast and take less time to complete, resulting in minimal changes in the concentrations of the reduced and oxidized species.

2.2.4. Screen Printed Electrodes

Recently, the progress in printing technology has enabled the economical manufacturing of disposable screen-printed electrodes (SPEs). SPE is a valuable technology that combines reference, working, and counter electrodes. They are frequently used in electrochemical test platforms because of their excellent properties. SPEs are disposable and portable electrodes, and they enable numerous experiments to be carried out with small amounts of samples [33].

The SPEs are fabricated using inks of gold, silver, and carbon materials. SPEs are commonly used for clinical analysis in medicine, pharmacy, agriculture, and environment. **Table 1** shows an overview of many studies based on the SPE.

Table 1. Overview of current research on screen-printed electrode-based studies.

Type of device	***Analyte***	***Specifications***	***Reference***
Screen-printed sulfide-selective sensor	Sulfide ions	Microfluidic platform, sensor design	[34]
Selenocysteine-modified screen-printed carbon nanofiber electrode	Trace metal ions	Selenium-based sensor design	[35]
Screen-printed electrodes coated with quaternized poly (4-vinyl pyridine) anion-exchange polymer	Sulfide	Indirect voltammetric method	[36]
Screen-printed electrochemical aptamer-based sensor	Chlorpyrifos (CPF)	Aptasensor design	[37]
Screen-printed electrode	Caffeic acid in wine samples	Portable sensor design	[38]

Pol et al. developed an electrochemical sensor to detect sulfide ions. This system combines screen-printing methodology for the fabrication of the sulfide-selective electrode with 3D printing techniques to create a compact and efficient potentiometric microfluidic platform. The integrated device offers several advantages, including portability, rapid response times, and high sensitivity to sulfide ions. The sensor performance was rigorously evaluated through experiments, demonstrating its capability to detect sulfide ions in various environmental and analytical applications precisely. This research represents a notable advancement in sensor technology, offering a versatile and practical tool for monitoring sulfide levels [34].

Chen et al. fabricated a microfluidic device bonding polydimethylsiloxane microfluidic channels onto an SPE substrate. This device is designed for prostate-specific antigen (PSA) electrochemical sensing. This device offers simplicity, quickness, cost-effectiveness, and scalability for mass manufacturing instead of traditional microfabrication processes. The developed microfluidic device successfully detected PSA in human serum [39].

Inam and colleagues produced an SPE-based electrochemical sensor. This sensor can detect chlorpyrifos (CPF) rapidly. Optimization of parameters, including aptamer concentration, pH, and incubation time, resulted in a brilliant performance for an aptasensor. The LOD was 0.097 ng/mL under optimal conditions. Stability over time was evaluated and resulted in good performance during the first 14 days, followed by a decrease in sensitivity due to aptamer degradation [37].

Zaguirre and colleagues have developed a voltammetric method to analyze drug iridium levels. The electrochemical experiments employed different types of modified SPEs, including graphite, carbon nanofibers, and carbon nanotubes, to detect low concentrations of Iridium. The SPCE modified with carbon nanotubes demonstrated the best LOD with a value of 0.03 mg/L [40].

2.3. Biosensors

Biosensors are powerful and compact analytical devices that convert biological signals into electrical signals [41]–[43]. They incorporate a biological sensing element across a broad range of applications, including drug discovery [44], [45], diagnostics [46]–[48], food safety and processing [49], environmental monitoring [50], etc. Other applications of biosensors are illustrated in **Fig. 2**.

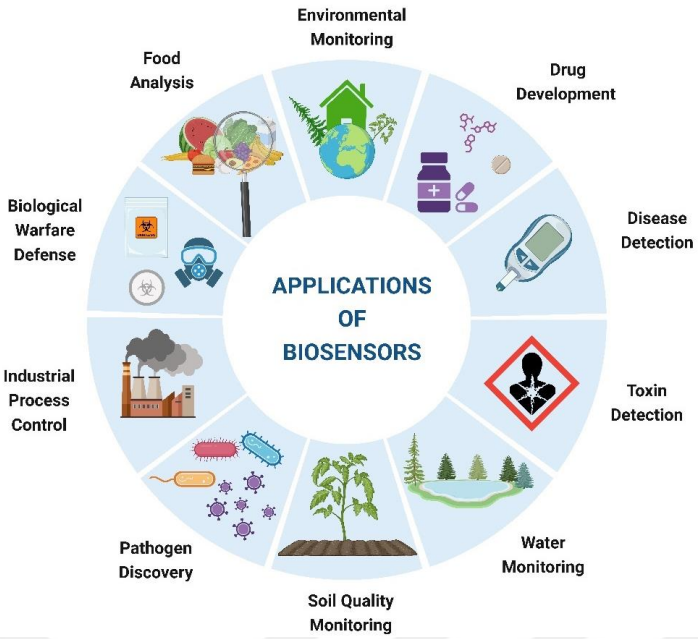


Figure 2. Applications of biosensors in various fields, including drug development, disease detection, pathogen discovery, and environmental monitoring. *It was created with BioRender.com.*

Biosensors consist of three main components (**Fig. 3**): an analyte, a bioreceptor and a transducer [41], [51]. A biorecognition element, also known as a bioreceptor, is a biocomponent capable of detecting a specific target analyte [52]. The transducer measures the biological signals and converts these biological signals into digital signals [53].

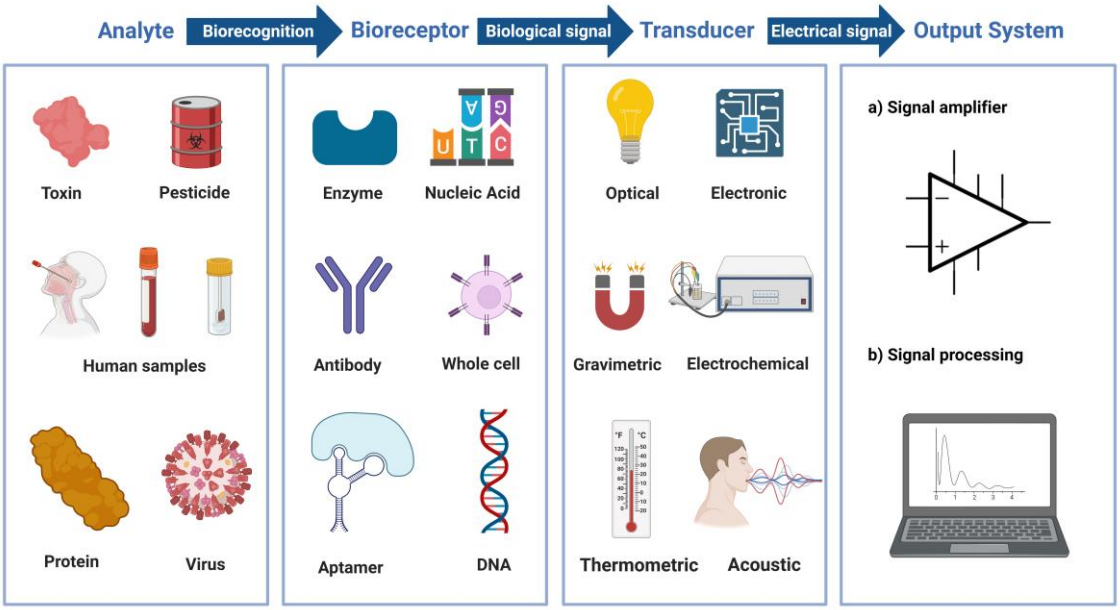


Figure 3. General schematic of a biosensor consisting of analyte, bioreceptor, and transducer [53]. *It* was *created with BioRender.com.*

Transducers are classified as electrochemical, optical, electronic, gravimetric, thermometric and acoustic based on their working principles. The output system amplifies and converts the electrical signals into digital form. They can be combined with nanowires, nanorods, metal oxide nanoparticles, and dendrimers as significant components in their design. Nanoparticles have raised the sensitivity and selectivity of biosensors [54], [55]. Biosensors can be subclassified based on various criteria, including the type of biological element, their operation principle and transduction method. According to the receptor types, biosensors can be divided into enzyme-based, antibody-based, cell-based, and nucleic acid-based biosensors. Enzyme-based biosensors integrate the specificity and selectivity characteristics of enzymes with the enhanced sensitivity of electrochemical sensing [56]. Clark and Lyons developed the first enzyme-based biosensor to monitor blood glucose levels [57]. Antibody-based biosensors detect the antigen-antibody binding, generating a specific readout signal [58]. Antibodies can bind to the surface of the sensor via affinity tags, covalent interaction, simple absorption, and entrapped [59].

Various cell types can be employed in the design of cell-based biosensors, including bacteria, fungi, algae, yeast, cancer cells, immune cells and neuronal cells. Cell-based biosensors can be employed in many areas, including clinical/health care (cell viability, proliferation, cell metabolism, cancer cell migration and biomarker characterization)[60], food safety (allergens, toxic compounds)[61], pharmaceutical (drug screening, chemotherapy effects, drug activity)[62] and environmental (water toxicity, biotoxicity)[63]. Nucleic acid-based biosensors utilize nucleic acid as a bioreceptor and a transducer to convert the biorecognition action into a measurable signal, as shown in **Fig. 4**.

Based on the detection system, biosensors can be subclassified as optical, electrochemical, and mechanical. In optical biosensors, the biosensing element and the optical transducer are integrated [64]. Optical biosensors enable real-time detection of numerous biological and chemical substances [65]. Optical biosensing can be used in two detection methods: label-based and label-free [66]. The label-free detection method generates the signal immediately when the studied material interacts with the transducer. Conversely, the label-based sensing method utilizes an identifier to generate an optical signal via a colourimetric, fluorescent, or luminescent technique [64]. Mechanical biosensors find widespread application in detecting diverse biomarkers [67]. They depend on properties that scale well as physical size decreases [68]. Additionally, their mechanical compliance allows the conversion of applied

force into discernible signal changes, offering novel avenues for quantifying the force involved in biomolecular interactions governing processes such as transcription and transport [69]. In electrochemical biosensors, during a biochemical reaction, signals generated by electrochemical species are converted into electrical signals that can be measured by a detector [70]. Electrochemical sensors have been used for a variety of applications including biomedical [71], environmental [72], [73], food [74], [75], and pharmacy [76]. Moreover, they are cost-effective, portable, and user-friendly, making them ideal for field applications [77]. They can be integrated into portable devices or smartphones [78], [79].

2.4. Development of DNA-electrochemical Biosensors

In recent years, notable progress in materials science, manufacturing technologies, and biomedical research has significantly influenced the evolution of electrochemical biosensor technology. Electrochemical sensor technology offers high sensitivity, cost-effectiveness, and rapid detection of the chemical reaction mechanism between pharmaceuticals and DNA [80].

A DNA-electrochemical biosensor comprises a transducer and immobilized dsDNA, also known as a probe. When immobilized DNA interacts with an analyte, it undergoes structural changes detected using a transducer (**Fig. 4**).

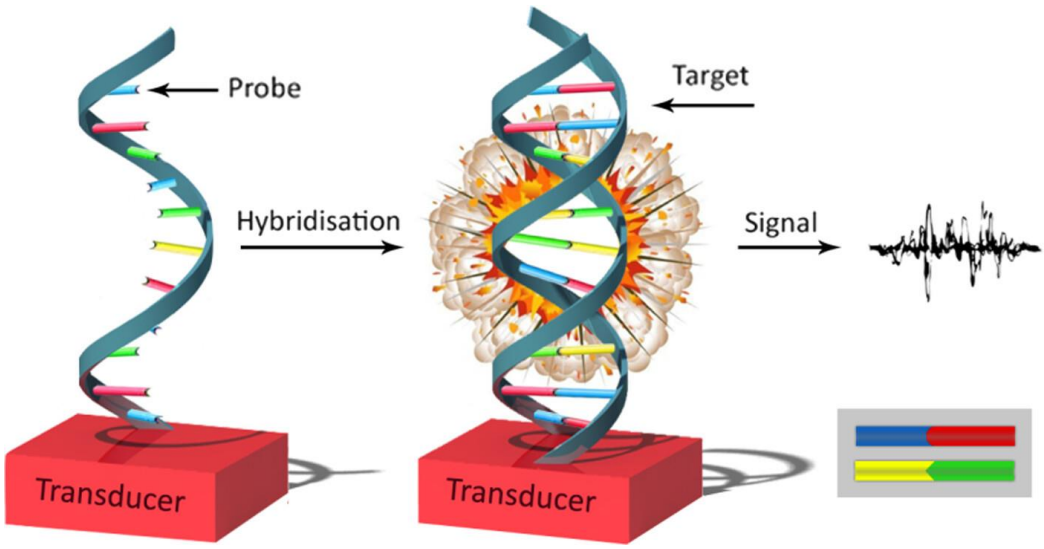


Figure 4. General schematic of the DNA-based biosensor [81].

The oxidation of purines (adenine and guanine) necessitates lower potentials, whereas pyrimidines (cytosine and thymine) demand considerably higher potentials. This determination

becomes challenging due to the proximity of these potentials to the oxygen evolution potential. Many DNA biosensors use guanine oxidation peaks to measure oxidative damage to DNA because guanine and adenine possess the lowest oxidation potential. Therefore, analyzing oxidative changes in DNA through purine bases is a more suitable approach. Oliveira-Brett and colleagues investigated the voltammetric oxidation of all DNA for the first time using a GCE. Based on the obtained results, the analysis of DNA base oxidation peaks indicates that guanine (G) exhibits the most easily oxidizable peak at 0.70 V. Subsequent peaks signify the oxidation of adenine (A) at 0.96 V, thymine (T) at 1.16 V, and cytosine (C) at 1.31 V [82].

The reduction of adenine and cytosine is irreversible, and the cathodic peak is observed at a notably negative potential, approximately around −1.4 V [83]. Conversely, the reduction of guanine occurs at a considerably negative potential.

2.5. Immobilization Techniques in Biosensors

The most common immobilization techniques in biosensor design are physical adsorption, covalent binding, cross-linking, entrapment and encapsulation.

2.5.1. Physical Adsorption

This technique attaches a bioreceptor to an inactive solid component via weak attractive forces [53], [84]. The physical adsorption approach provides many advantages, such as ease of use, affordability, minimal impact on bioreceptor activity, and lack of requirement for changing biological components or producing a matrix [85]. However, there are a few disadvantages to this approach. These variations influence this method in the pH level, temperature, and concentration of ions.

2.5.2. Covalent Binding

The bioreceptor generates a strong bond with the non-reactive matrix in the electrode/transducer surface in this technique. Utilizing covalent binding provides numerous advantages, such as more excellent resistance to environmental fluctuations, reduced enzyme leakage, and the creation a strong bond. On the other hand, this approach has several disadvantages, most notably the employment of harsh chemicals and the irreversible nature of the matrix after usage [53], [86], [87].

2.5.3. Cross Linking

Cross-linking is the process that generates covalent bonds between molecules, either between biorecognition elements (enzymes) or essentially inert proteins. Enzyme molecules are connected into three-dimensional cross-linked clumps on the transducer surface by multifunctional reagents serving as linkers. Precise pH level, temperature, and ionic strength control is required to achieve ideal cross-linking conditions. Strong attachment, accelerated reaction rates, and increased enzyme catalytic activity are advantages of this technique [85], [88].

2.5.4. Entrapment

Enzymes are trapped within a polymeric network in the capture immobilisation technique, preventing direct binding to the support surface. This process reduces leaching and denaturation while increasing the stability of the enzymes. The procedure involves the dissolution of the enzyme in a monomer solution. A polymerization process is followed, and the physical restriction within the polymer framework enables enzyme microenvironment optimization. There are also disadvantages, such as the possibility of degradation of the support material during polymerization, poor enzyme loading capacity, possible leakage if the support matrix holes are too broad, and mass transfer resistance introduced by thicker gel matrices. Depending on the type of entrapment, various techniques are used, such as microencapsulation, sol-gel, photopolymerization, and electropolymerization [89].

2.5.5. Encapsulation

The encapsulation technique is cost-effective and straightforward, enclosing biological recognition elements in a spherical membrane. In this technique, various types of membranes, including polymeric membranes, lipid membranes, and non-ionic membranes, can be employed. Also, this technique incorporates two distinct processes. These two processes are the phase separation of enzyme microdroplets in liquid phases and polymerization between two insoluble materials [53].

2.6. Deoxyribonucleic acid (DNA) Structure

DNA plays a vital role in storing, reproducing, and transmitting genetic information [90].

It is a double-stranded structure composed of molecular building blocks called nucleotides. The DNA backbone is formed by the phosphate-deoxyribose sugar polymer (**Fig. 5**). Genetic information in cells is encoded by the purine bases (adenine and guanine) and the pyrimidine bases (cytosine and thymine) arranged consecutively in the chain. DNA is a common drug target that transports our genetic information.

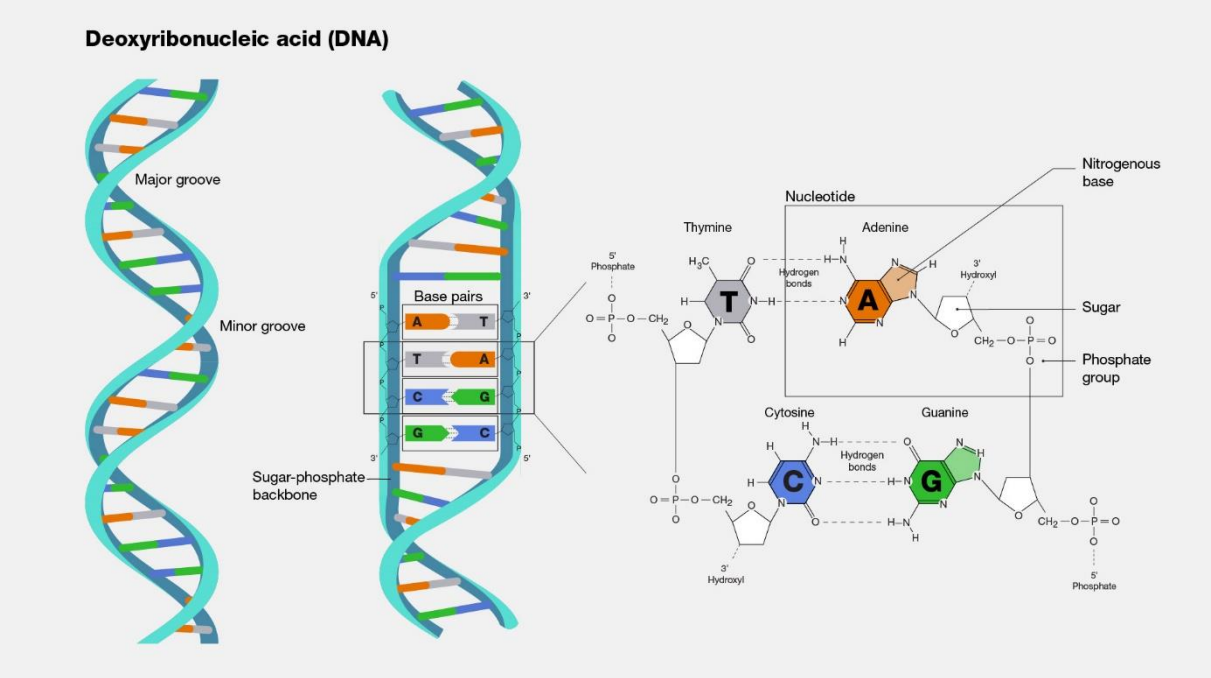


Figure 5. The DNA structure consisting of nucleotides (A, Adenine; T, Thymine; G, Guanine; and C, Cytosine)[91].

2.7. Types of DNA-drug Interaction

The interaction of drugs and DNA constitutes an important step for pharmaceutical development. The interactions between drugs and DNA are of two types: covalent and non-covalent bindings. Covalent binding between drug and DNA is permanent and causes inhibition of DNA functions. On the other hand, non-covalent binding involves a reversible mechanism that is further classified as intercalation, electrostatic interactions, and groove binding. Intercalation is an interaction where small molecules bind to DNA from specific regions [92]. Electrostatic binding results from unspecific stacking interactions among specific ligands and negatively charged DNA phosphate groups. Small molecules interact with DNA via its minor groove through relatively weak bonds, a phenomenon known as groove binding [93].

Drug–DNA interactions can be determined using instrumental methods, including optic spectroscopy, viscosity measurements, mass spectrometry (MS), and electrochemical techniques [94]–[97]. Among them, electrochemical techniques are the most essential because of their simplicity and quickness [96]. Electrochemical techniques provide a simple, low-cost, and time-efficient way to analyze drugs with low detection limits compared to other methods [98].

Wang and colleagues investigated the effects of the antitumor drug Daunomycin on dsDNA. This study utilized voltammetric techniques with CPE to explore the interaction in solution as well as electrode surface. These electrochemical techniques provided information about Daunomycin's electroactive behaviour and binding affinity [99].

Karimi-Maleh and co-workers produced an electrochemical biosensor using ds-DNA as the bioreceptor on GCE enhanced with Pt/SWCNTs nanocomposite. The intercalation interaction among the anticancer chemotherapeutic drug Daunorubicin and dsDNA was examined, particularly on the guanine signal. The results obtained from DPV indicated a linear dynamic range with a LOD of 1.0 nM [100].

Kurbanoglu and colleagues studied the interaction of Aripiprazole (ARP) with dsDNA. The DPV method and UV–VIS spectrophotometry were performed to understand the interaction of ARP with calf thymus dsDNA on GCE. The binding constant (K) value among dsDNA and aripiprazole was $3x10^5$ M^{-1} [101].

2.8. Drug Candidate Molecules

Triazolopyrimidinones are considered a privileged core in medicinal chemistry. Heterocyclic compounds, which include five- and six-membered nitrogen-containing aryl substituents, have gained considerable interest due to the discovery of their effects in chemistry [102]. In this context, triazolopyrimidinone has been reported to have various activities involving anticancer, antimicrobial, antifungal, herbicide, antitumor, and antioxidant properties [103].

In the literature, numerous papers discuss the activity of triazolopyrimidinone and its derivatives. Lan et al. identified triazolopyrimidine derivatives as selective FABP4/5 inhibitors and evaluated them for antifungal and apoptotic effects. They proposed that FABP4/5 inhibitors improve dyslipidemia in mice [104].

Ortiz Zacarías et al. assessed the biological activity of several triazolopyrimidinone derivatives targeting CC chemokine receptors 2 (CCR2) and 5 (CCR5). They demonstrated that molecule 39 and molecule 43 exhibit a non-competitive inhibition on CCR2 and CCR5 [105].

Moreau et al. discovered novel compounds targeting phosphopantetheine adenylyltransferase (PPAT) in Gram-negative bacteria. Triazolopyrimidinone 53 and azabenzimidazole 54 effectively blocked PPAT in E. coli and P. aeruginosa [106].

In another study, Hassan et al. synthesized various types of 1,2,4-triazolopyrimidine and 1,2,4-triazoloquinazoline compounds, denoted as compounds 6, 11, 26, 29, 41, 44, 48, 49, and 58. In vitro DNA-binding experiments and in vivo anticancer tests on mice were carried out to evaluate their potential antitumor activities. From these results, the strongest affinity for DNA was demonstrated by compound 26 in DNA binding assays. Compound 26 exhibited the highest level of activity (IC_{50}= 47) according to the colourimetric assay (Methyl green-DNA displacement assay). The authors concluded that the antitumor activity was enhanced by morpholine and phenylazo groups [107].

3. MATERIALS AND METHODS

3.1. Type of the Study

This thesis study is conducted as an experimental research.

3.2. Time and Location of the Study

The drug candidate molecules were synthesized at Izmir Katip Celebi University, Faculty of Pharmacy, between May 2022 and July 2022. All experiments were carried out between August 2023 and April 2023 at Izmir Biomedicine and Genome Center.

3.3. The Universe and Sample of Research

The drug candidate molecules were used in this study.

3.4. Working Materials

3.4.1. Apparatus and Instruments

An analytical balance of the KERN ABT 220-5DM (KERN, Germany) brand was employed for sample preparation. A desiccator and an oven were utilized in the PDMS preparation process. A Hanna brand pH Meter was employed to prepare the solution. All electrochemical measurements (DPV and CV) were conducted using a PalmSens4 potentiostat analyzer. It is connected to a personal laptop using a Universal Serial Bus (USB cable) and is controlled through our C# based software. A three-electrode setup was used, including a PGE working electrode, an Ag/AgCl reference electrode (3M NaCl), and a platinum wire counter electrode (7.5 cm). A thermal shaker (Thermo Fisher Scientific) was used to prepare the solution. SPEs were used to validate the three-electrode system-based interaction experiments. SPES (DS110) were purchased from DropSens, Spain.

3.4.2. Chemicals

All chemicals were purchased from Sigma-Aldrich (USA) and Thermo Fisher Scientific (USA) and were used without further purification. SYLGARD™ 184 Silicone Elastomer Kit was used for PDMS production.

3.4.3. Synthesis of Drug Candidate Molecules

Drug candidate molecules, triazolopyrimidinone derivatives, were synthesized and referred to as ((5-(Chloromethyl)-2-(4-methoxyphenyl)-[1,2,4]triazolo[1,5-a]pyrimidin-7(3H)-one) **(D_1-TP)**, 2-(4-Methoxyphenyl)-5-(piperidinomethyl)-[1,2,4]triazolo[1,5-a]pyrimidin-7(3H)-one **(D_2-TP)**, and 2-(4-Methoxyphenyl)-5-(morpholinomethyl)-[1,2,4]triazolo[1,5-a]pyrimidin-7(3H)-one **(D_3-TP)** [108]. **Fig. 6** shows the chemical structures of D_1-TP, D_2-TP and D_3-TP.

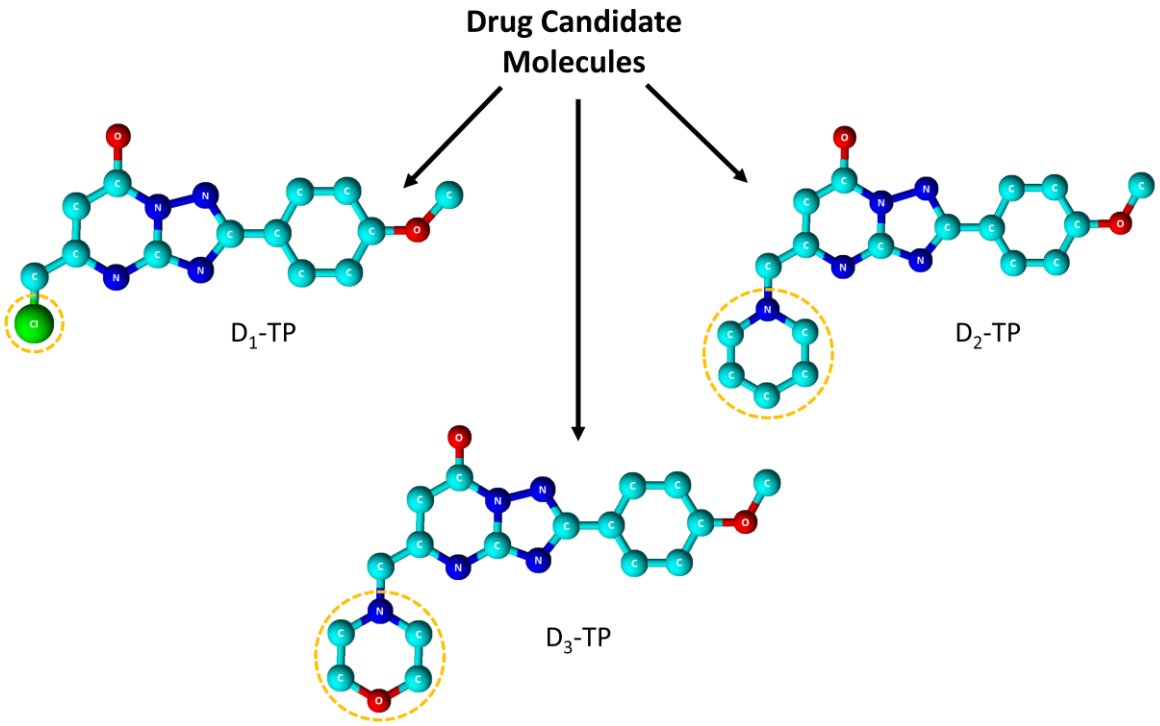


Figure 6. Chemical structure of drug candidate molecules: D_1-TP, D_2-TP and D_3-TP.

The synthesis of pyrimidinone-triazole derivatives is in this protocol [109].

3.5. Optimization Study of Drug Candidate Molecules using a Three Electrode System

The synthesized drug candidate molecules were optimised using a three-electrode system (**Fig. 8**). All electrodes were soaked to sample solution in a glass cell. Before all experiments, PEGs were cut to lengths of 3 cm. The PGE surface was then activated using a +1.4 V potential for 30 seconds (**Fig. 7**). Electrochemically activated PGEs were employed as working electrodes for further experiments. Pretreated PGEs offer several advantages compared to non-pretreated PGEs, including enhanced surface area and increased active sites. Those factors accelerate electron transfer at the electrode surface [26].

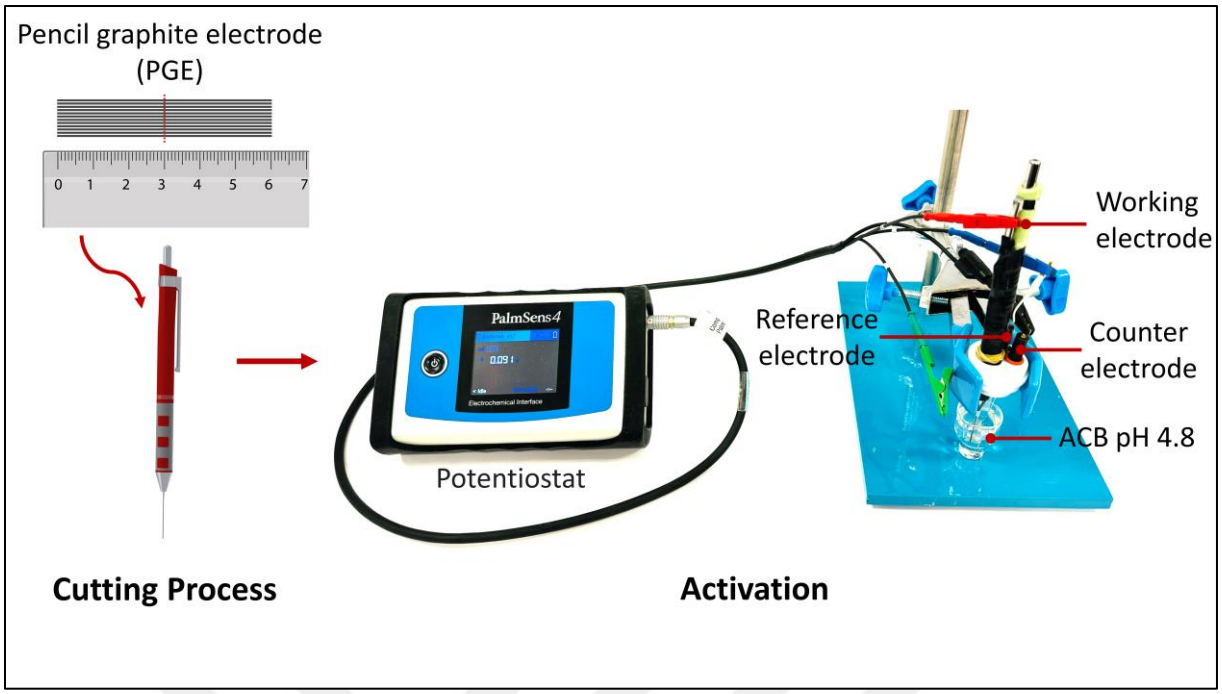


Figure 7. Activation process of PEGs: PEGs were cut into 3 mm lengths and activated by applying +1.4 V for 30 seconds in ACB at pH 4.8.

After activation, parameters of drug candidates, such as pH, scan rate, and concentration, were optimized. Additionally, stability tests of drug candidates were performed on different days. Subsequently, their interactions with dsDNA were examined.

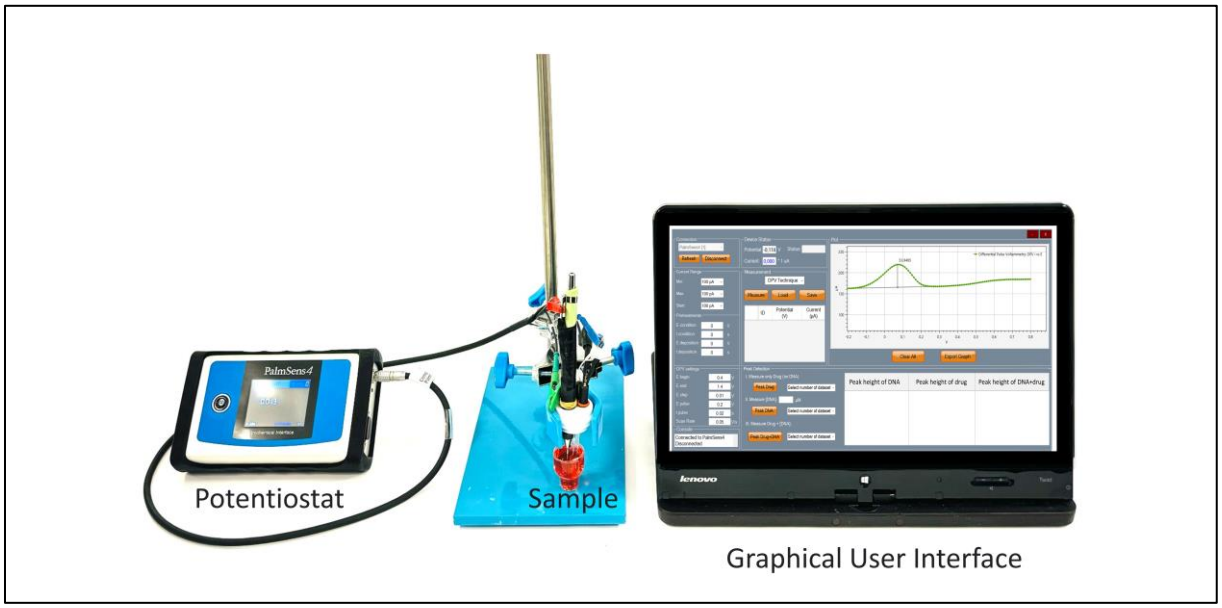


Figure 8. The experimental setup consisted of a PalmSens operating as a potentiostat, a three-electrode system, and a graphical user interface.

3.5.1. Optimization of pH

Determining the optimum working pH is crucial for understanding the therapeutic effects of drug candidates. The oxidation signals of Ds-TP were investigated over a pH range of 3.8 to 7.4. DPV measurements were performed by applying the potential between 0.4 and 1.6 V. The ingredients of the buffer solutions used for different pH values are shown in Table 2.

Table 2. The ingredients of the buffer solutions for different pH values.

Buffer Solution	**pH**	**Ingredients**
Acetate buffer (ACB)	4.8	20 mM NaCl, 0,5 M Glacial acetic acid
Tris buffer (TBS)	7.0	20 mM NaCl and 20 mM Tris-HCl
Phosphate buffer (PBS)	7.4	20 mM NaCl, 50 mM Phosphate (KH_2PO_4 and K_2HPO_4)

3.5.2. Optimization of Drug Concentration

The DPV technique was used to apply the potential between 0.4 and 1.6 V to determine the analytical concentration ranges of Ds-TP. The Limit of Detection (LOD) for Ds-TP was calculated across the concentration range of 2.5 to 20 μg/mL.

3.5.3. Scan Rate Study

Essentially, the scan rate influences the efficiency of the electrochemical reactions by affecting the kinetics of mass transport at the electrode interface. Increased scan speeds cause the diffusion layer to decrease, which raises the detected currents [8]. The CV method investigated the effect of varied scan rates (V) on peak current (Ip) between 25 and 150 mV/s.

3.5.4. Stability Study

Stability is an intricate factor that is related to the efficacy of drug candidates [110]. It

affects pharmaceutical development, identity, strength, purity, and quality. DPV measurements were performed by applying the potential between 0.4 and 1.6 V. Freshly prepared solutions of Ds-TP were kept in a dark room (25 °C). These solutions were measured on days 0, 5, 7, 14, and 30 to assess their stability.

3.5.5. Interaction Study with dsDNA

Examining the interplay between drug candidate molecules and DNA is essential for determining optimal drug dosages in disease treatment [111]. Additionally, exploring DNA-drug interactions contributes to developing innovative drug designs [112]. The stock solution of dsDNA was prepared using Tris-EDTA (TE) buffer (pH:8.0). The Ds-TP were initially dissolved in Dimethylformamide (DMF) to obtain stock solutions, which were subsequently diluted with ACB. Each solution of the drug molecule was mixed with dsDNA solution in a 1:1 ratio. The ultimate dsDNA concentration was set to 50 µg/mL. Additionally, the Ds-TP concentration was obtained at 10 µg/mL. A thermal shaker stirred them at 600 rpm for 30 minutes (45 °C). 100 µL of the mixture into small Eppendorf tubes. Then, the activated electrodes were placed into these tubes (**Fig. 9**). After 30 minutes, the surface of the electrodes was dipped once into a blank ACB buffer solution. After that, DPV measurements were performed by applying the potential between 0.4 and 1.6 V.

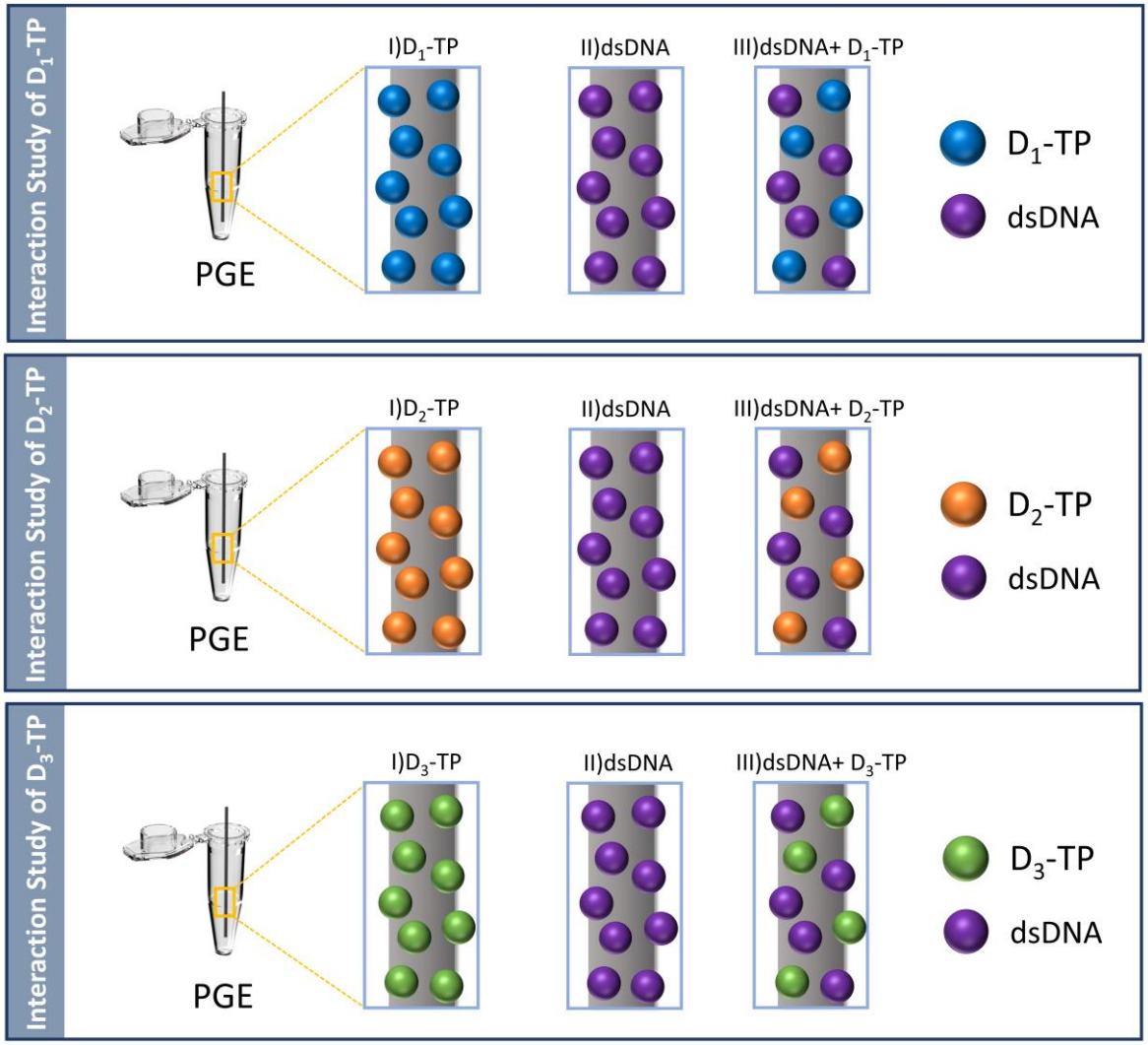


Figure 9. Investigation of the interaction between D_1-TP, D_2-TP, and D_3-TP with dsDNA, respectively.

The DPV technique was used within the potential between 0.4 and 1.6 V. The oxidation signals of dsDNA bases (guanine and adenine) were obtained after interaction with Ds-TP. Oxidation signals corresponding to DNA guanine bases were obtained at around 1.0 V.

3.6. Comparative Studies Using Screen-Printed Electrode-based Electrochemical Biosensor

After conducting optimization studies with the three-electrode system, the interaction of the Ds-TP with dsDNA was examined using an SPE (**Fig. 10**). The SPE is a portable electrode that integrates three components: a WE, a RE, and a CE.

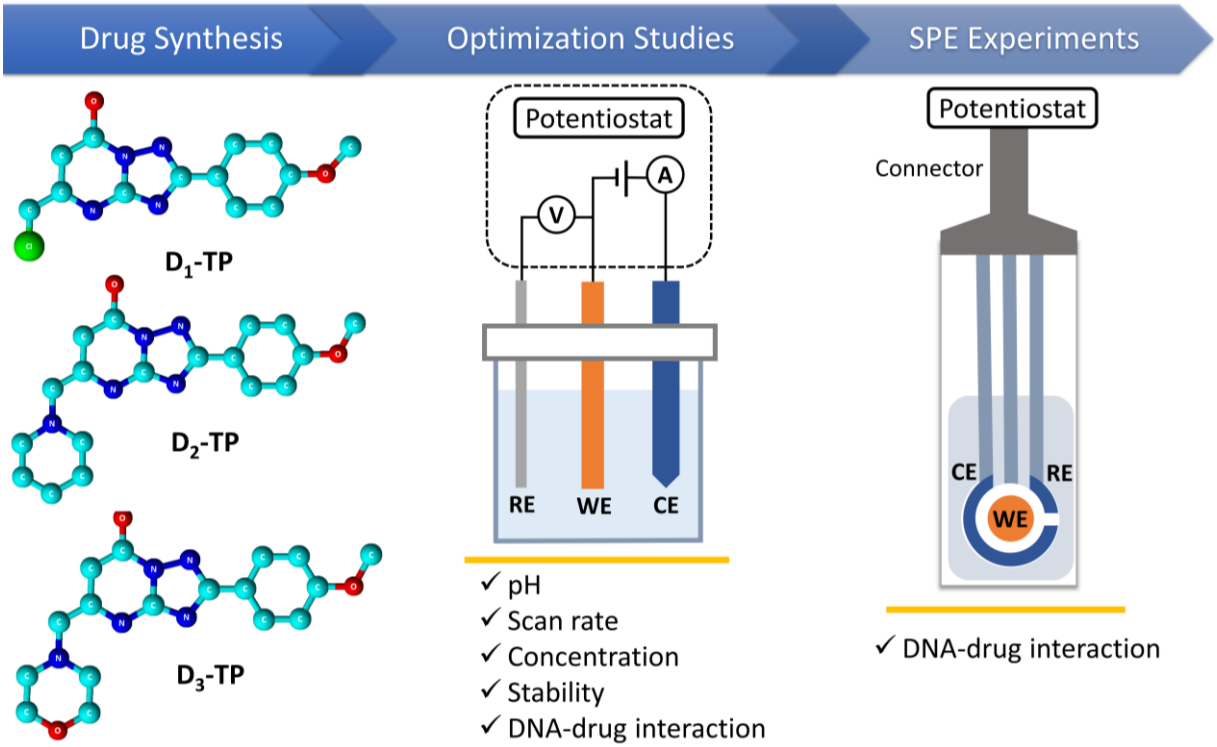


Figure 10. The general scheme of this study includes drug synthesis, optimization studies with a three-electrode system, and DNA-drug interaction tests with SPE.

The SPE was integrated into an electrochemical biosensor system. Portable electrochemical biosensors were developed consisting of two acrylic caps separated by two PDMS layers. This biosensor comprises three sample chambers dedicated to DNA, DNA + drug, and drug configurations.

3.6.1. Development of Electrochemical Biosensor Platform

The electrochemical biosensor platform comprises a sample apparatus, potentiostat and graphical user interface. It is designed with a sample apparatus for easy measurements, including two sealing layers made of PDMS layers and two acrylic locking caps. Additionally, a 3D design of PDMS molds containing a sample chamber to cover the working areas of the SPE was created using the SolidWorks design program. A biocompatible and non-toxic elastomer, PDMS, was used to fabricate the sample apparatus. The PDMS-based sample holder features three circular sample chambers designed for the placement of DNA, DNA+drug, and drug samples, ensuring uniform distribution over the surface of the SPE (**Fig. 11**). The design specifications, including dimensions and depths, were meticulously defined for optimal

functionality. Resin-based molds were designed to serve as negative molds for creating PDMS layers.

These parts were saved in .stl file format and then transferred to the Formlabs resin printing device through the " Preform interface." The components were successfully produced with an enhanced filling ratio and under suitable ventilation conditions using a Stereolithography (SLA) 3D printer. Subsequently, the obtained molds were filled with PDMS. In this context, the following steps were followed:

I. The elastomer and polymerization agent were blended (10:1 ratio) until transparent. The resulting liquid PDMS was poured over the negative molds.

II. Then, molds were vacuumed for 1 hour to eliminate air bubbles.

III. Afterwards, the filled molds were polymerized in an oven for 1 hour (70°C).

IV. The polymerized PDMS, with a channel structure, was carefully removed from the mold using a scalpel.

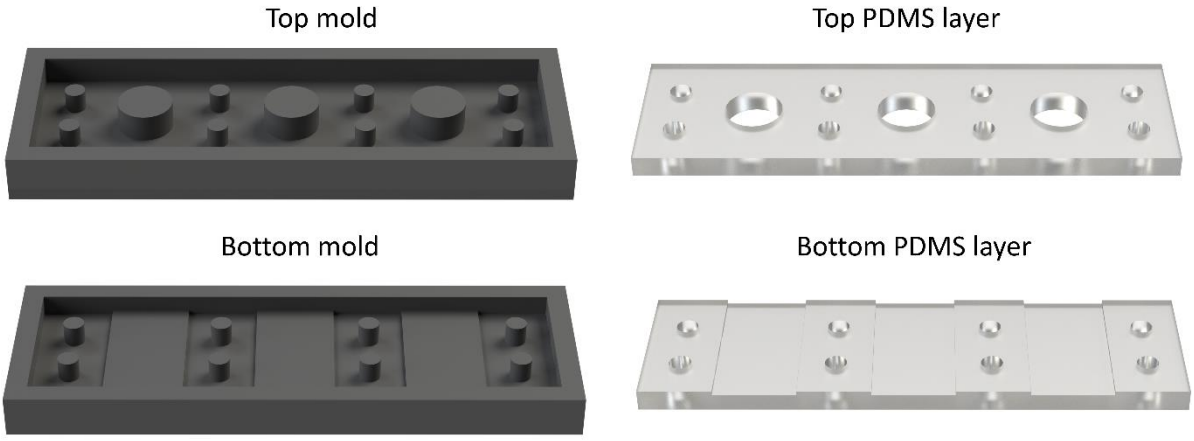


Figure 11. The bottom and top resin-based molds and PDMS layers.

The acrylic locking caps were designed in SolidWorks to fit PDMS materials, and the design details were saved in .dxf format. These .dxf files were then transferred to CorelDRAW, which served as the interface for the laser-cutting device. The cutting process was accurately executed in CorelDRAW. The acrylic locking caps were efficiently crafted from acrylic sheets using these steps. The sample holder assembly was obtained by assembling PDMS layers and acrylic caps sequentially, with the SPEs positioned in the middle (**Fig. 12**).

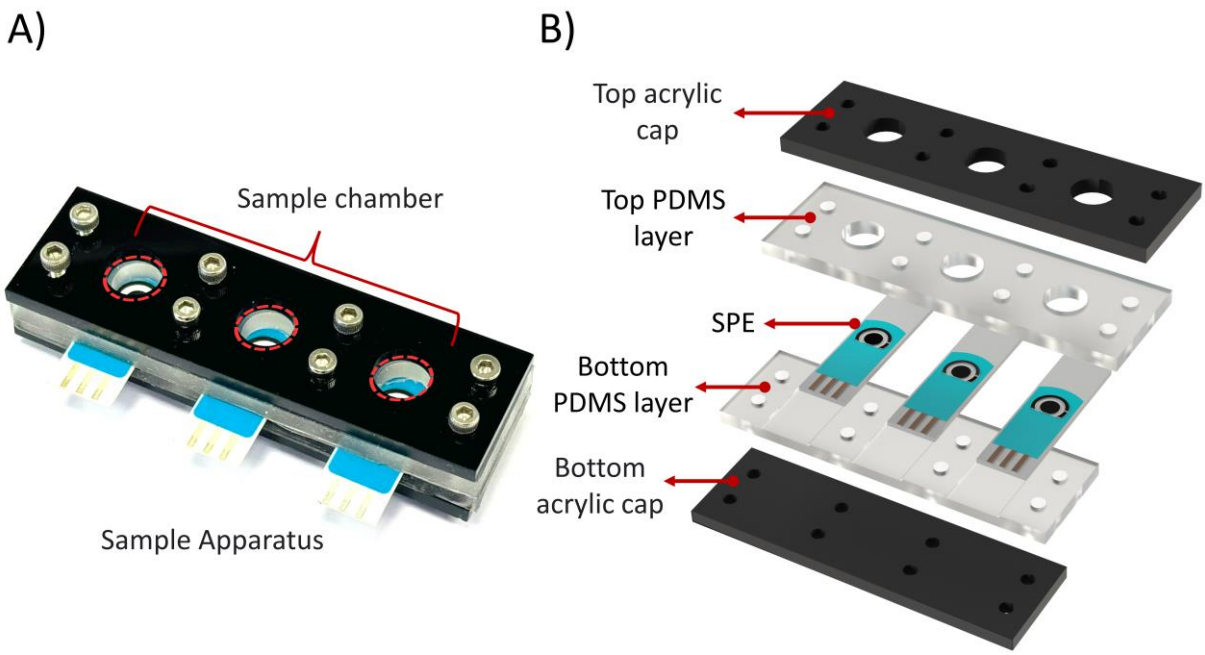


Figure 12. In the photograph of the sample apparatus (A), SPEs were sandwiched between PDMS layers, which were then inserted between two acrylic caps (B).

3.6.2. Graphical User Interface (GUI)

C#-based GUI was developed to enhance the functionality and flexibility of PalmSens4 electrochemical measurement devices, facilitating the processes of data collection, analysis, and reporting. While the PalmSens4 device is equipped with its own PSTrace software featuring a more complex interface, our GUI is specifically designed to process and record data related to DNA-drug interactions. The GUI of the platform is developed on Microsoft Visual Studio using the C# language. **Fig. 13** displays the main panel of the GUI. The open-source PalmSens4 Software Development Kit (SDK) was integrated into GUI for electrochemical analysis to control the selected potentiostat. This integration allows effective control of PalmSens4 measurement tools. The communication protocol used for interaction between the GUI and PalmSens4 is serial communication. GUI consists of 6 main panels: Connection, Device Status, Plot, Measurement, Settings, Console and Peak Detection panel.

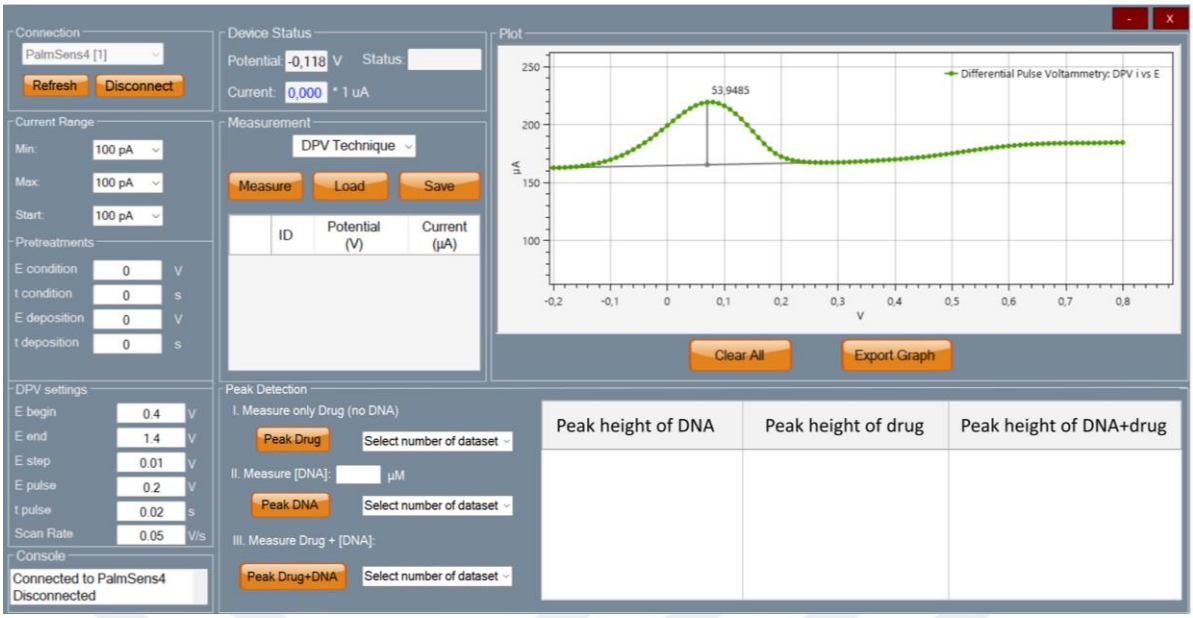


Figure 13. Graphical user interface.

- **Connection Panel:** This panel is used to connect devices. When the "Refresh" button is pressed, connected devices are displayed on the screen. The "Connect" button establishes a connection with the selected device.
- **Device Status Panel:** It displays the real-time measured voltage and current values, as well as the status of the device.
- **Plot Panel:** It shows the measurement results as a Potential (V) versus Current (µA) graph on the screen. The "Clear All" button clears the current graph, and the "Export Graph" button saves the graph to the selected folder.
- **Measurement Panel:** This panel enables the operator to perform a variety of measurements using different techniques from PalmSens4, such as CV and DPV. After selecting the measurement method, the necessary parameters for each method are displayed on the screen. The settings for each selected method are found in the left panel. The "Measure" icon initiates the chosen measurement. The "Load" icon loads the previous measurement into the interface. The "Save" button saves the measurement result and method used. The desired current value can be selected in the "Current Range" section. The main settings of the selected method are entered in the lower part, called the settings panel.
- **Console Panel:** This panel shows the status of connected devices and a list of operations performed on the interface.

- **Peak Detection Panel:** This panel saves the peaks in measurements of DNA, DNA+Drug, and drug, displaying the results in the right panel.

3.6.3. Testing Procedure

The measurement of Ds-TP at the dsDNA-modified SPEs consisted of four crucial steps: treatment of the electrode surface to increase its hydrophilicity, dsDNA immobilization to interact with the drug candidates, and subsequent interrogation of the electrode surface.

In detail, the steps of the experiment were as follows:

- *Pre-treatment:* Before experiments, all SPEs were activated using a potential of 1.8 V for 1 minute under stirred conditions. Activation of the SPE improves electroconductivity, electroactive surface area, and adsorptive characteristics [113], [114].
- *DNA immobilisation:* Sample solutions were prepared as described in **Section 3.5.5.** The surface of SPE was coated with 150 µL of the mixture (**Fig. 15**). Then, the electrode surface was rinsed with ACB.
- *Measurement:* After incubation, DPV measurements were carried out (**Fig. 14**). DPV parameters: potential range = 0.4 to 1.4 V, E_{Step} = 10 mV, E_{Pulse} = 200 mV, and scan rate = 50 mV/s.

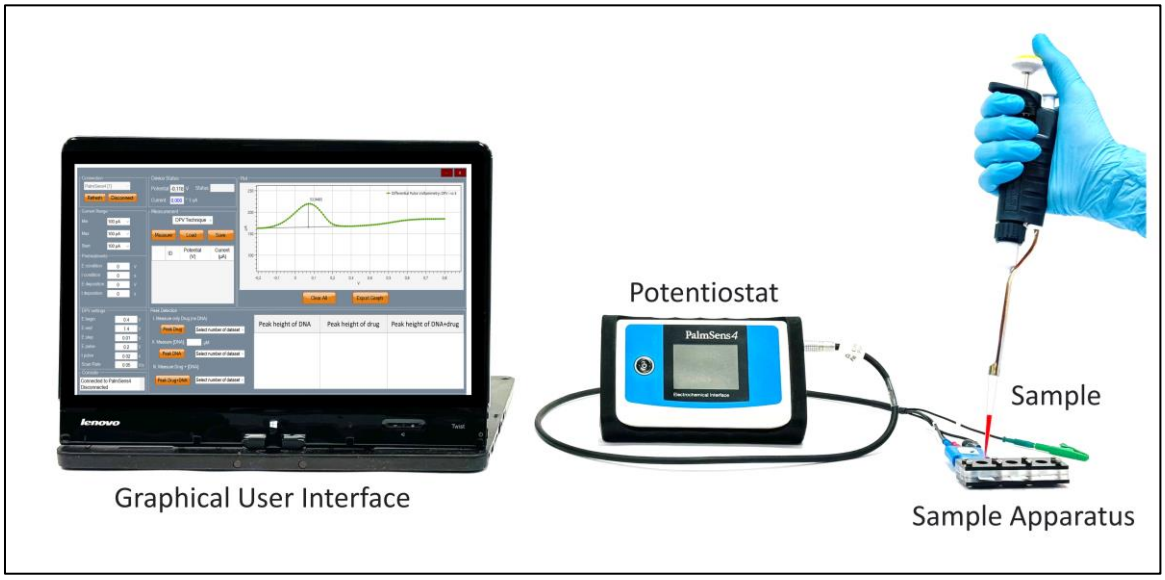


Figure 14. The general figure of electrochemical biosensor.

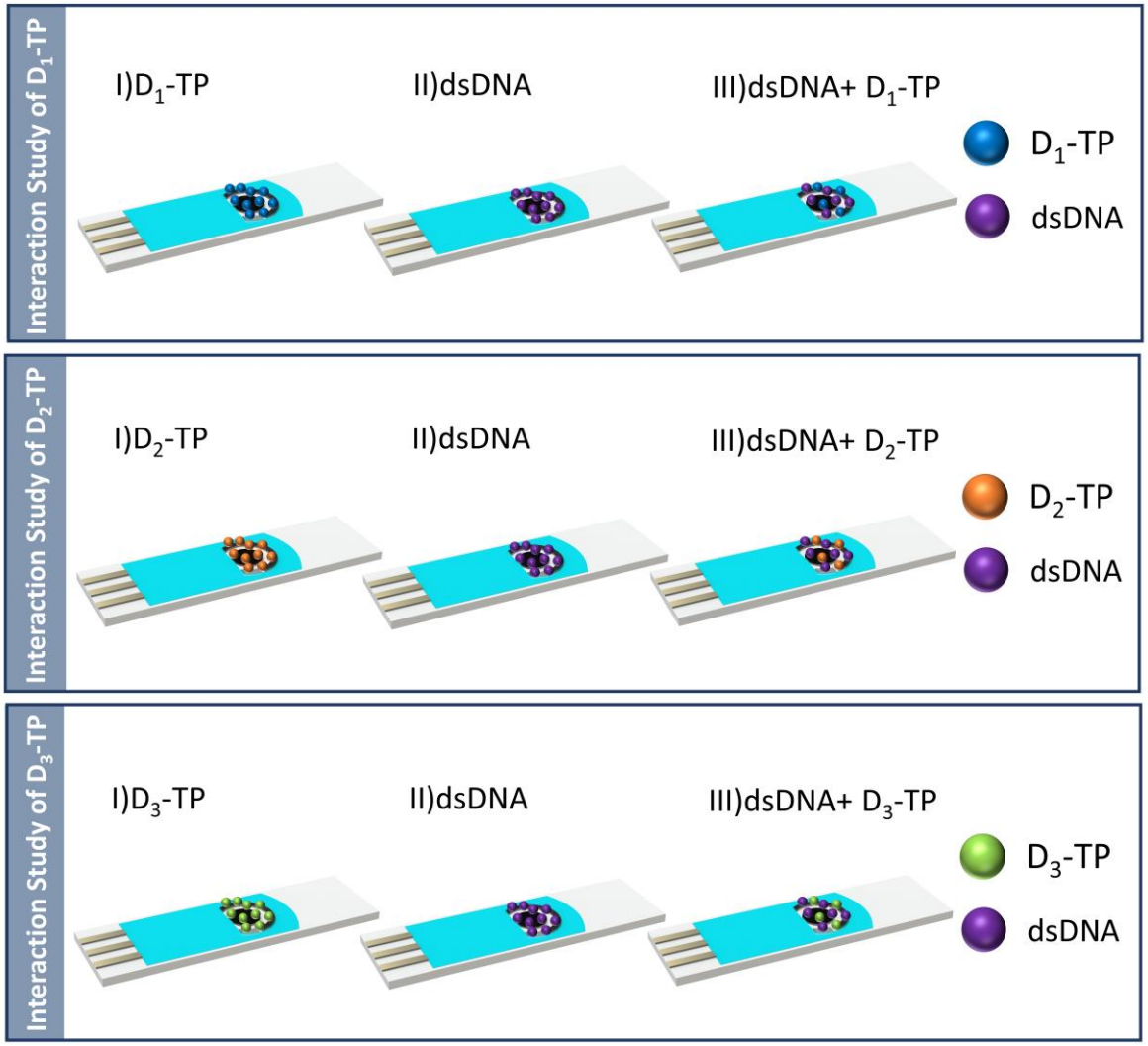


Figure 15. Schematic presentation for electrochemical detection of Ds-TP interaction with dsDNA using screen-printed electrodes.

3.7. Data Collection Tools

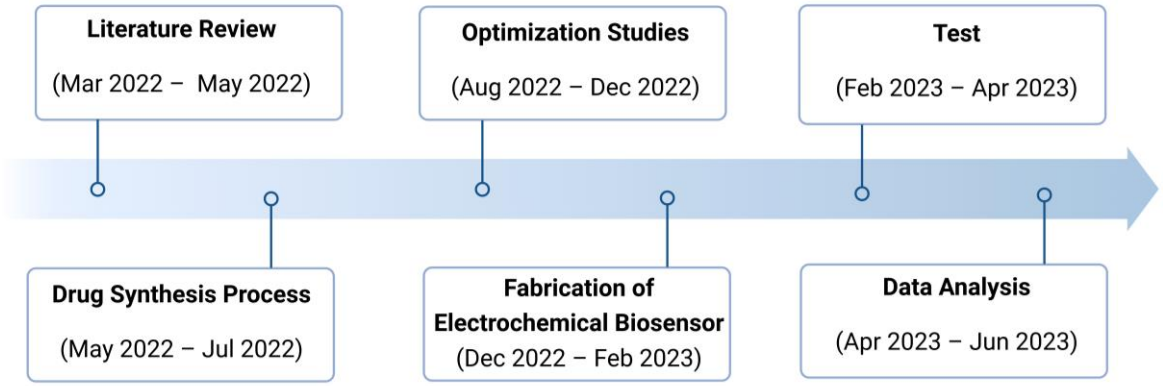
The PalmSens4 (BASi, US) potentiostat analyzer was used to obtain DPV and CV measurements. Technical specifications of PalmSens4 are shown in **Table 3**.

Table 3. Technical specifications of PalmSens4.

DC Potential Range	Between ±5 V and ±10 V
Compliance Voltage	±10 V

Maximum Current	±30 mA
Maximum Acquisition Rate	$15x10^4$ points/s
Electrode Connections	RE, WE and CE
Communication	USB and Bluetooth

3.8. Research Plan



3.9. Data Evaluation

Data were analyzed and plotted using GraphPad software (GraphPad Prism 8 Software, La Jolla, California, USA).

3.10. Limits of Study

This study has some limitations. First, the three-electrode system used in electrochemical-based analyses consists of reference, working, and counter electrodes, a glass measurement cell and connecting cables within a transformation mechanism. This three-electrode system's accurate and repeatable integration and connecting cables into the setup are crucial for precise measurements. However, the movement of electrodes throughout the experiment may result in noise signals in the transformation system, leading to errors in the evaluation of data obtained from measurements and affecting the reliability of the test results.

The three-electrode system used in studies requires a high level of skill and usage experience, leading to different electrochemical data for the same research conducted by other users. This variability poses a challenge to the parameter of repeatability in research.

Moreover, the lack of isolation of the measurement cell from the experimental environment makes it susceptible to external influences, introducing errors in the experimental results. For these reasons, screen-printed electrode was preferred in the electrochemical biosensor platform. As a part of the system, the screen-printed electrode provides a user-friendly and efficient solution, facilitating ease of use and enhancing the overall performance of the biosensor platform. Its selection is also attributed to its contribution to enhanced repeatability, ensuring consistent and reliable results across multiple experiments.

4. RESULTS AND DISCUSSIONS

4.1. Effect of pH

GraphPad Prism 8 Software was used for all statistical analyses. All values were presented as average ± standard deviation (SD).

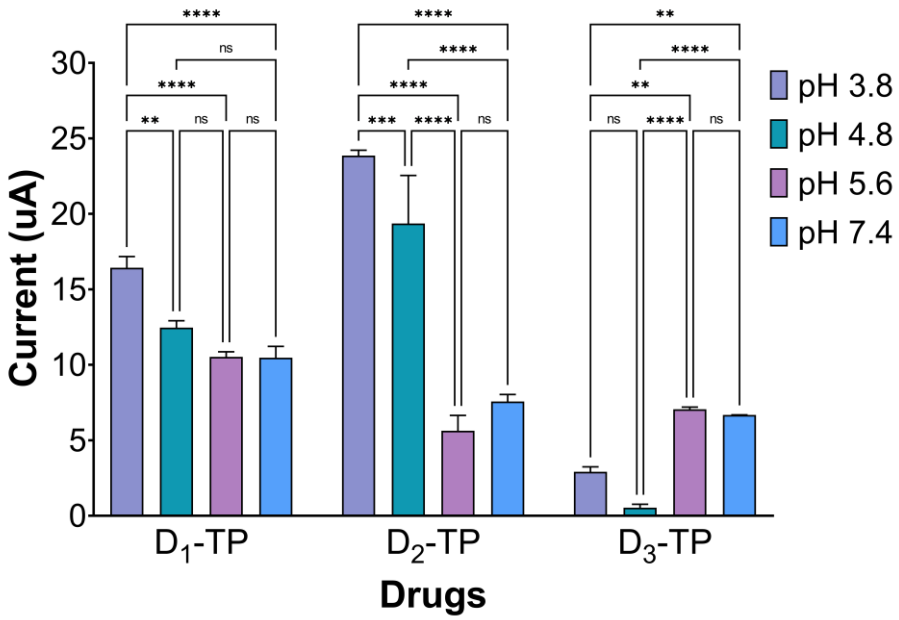


Figure 16. The effect of pH on peak currents of Ds-TP. The bar graph depicts drug candidates with a pH of 3.8–7.4. Error bars represent standard deviation (ns, not significant).

In **Fig. 16**, stable responses and the highest currents were observed for D_1-TP and D_2-TP at pH 3.8. D_3-TP produced a stable peak current at pH 5.6. Consequently, a dilution buffer of pH 3.8 was chosen for D_1-TP and D_2-TP and pH 5.6 for D_3-TP.

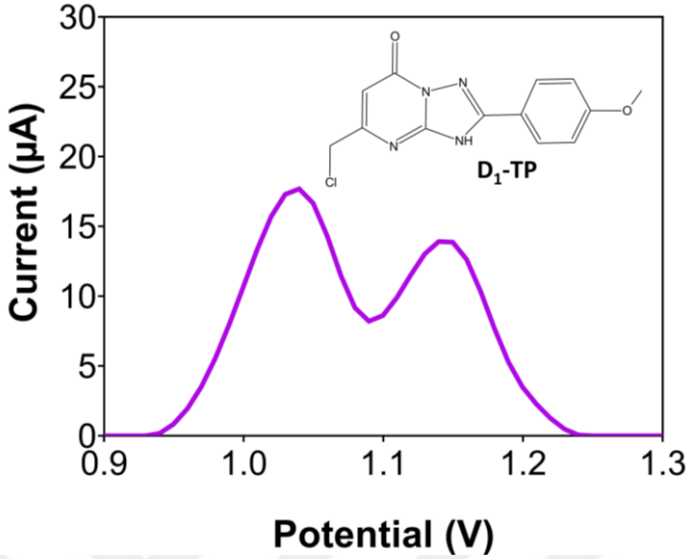


Figure 17. The DPV voltammogram of D_1-TP (ACB, pH 3.8). D_1-TP displayed oxidation peak potentials at 1.04 V and 1.14 V. (*The DPV voltammogram represents the result of a single measurement.)

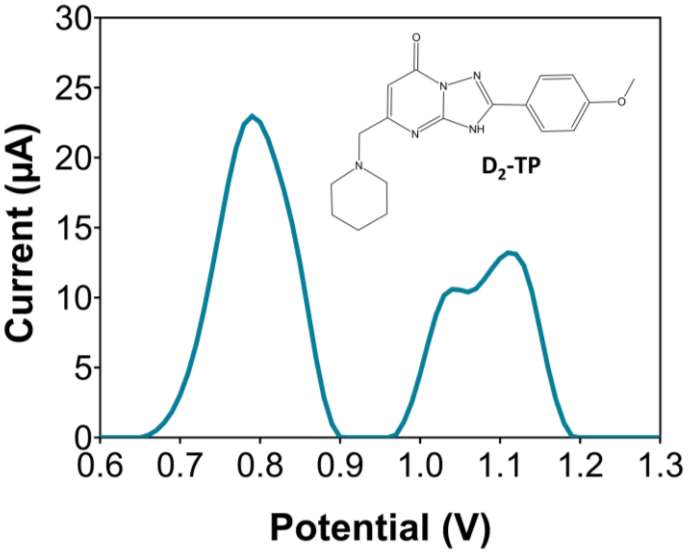


Figure 18. DPV voltammograms of D_2-TP (ACB, pH 3.8). D_2-TP showed two peak potentials at 0.79 and 1.10 V. (*The DPV voltammogram represents the result of a single measurement.)

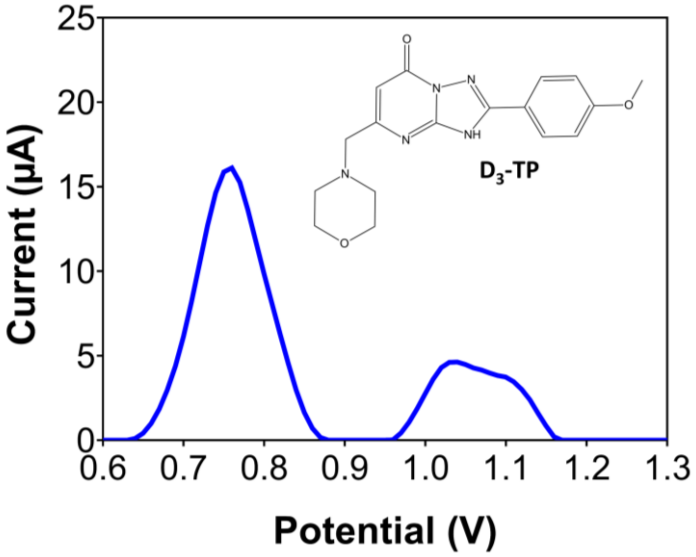


Figure 19. DPV voltammograms of D_3-TP (ACB, pH 5.6). D_3-TP exhibited two peak potentials at 0.76 V and 1.05 V. (*The DPV voltammogram represents the result of a single measurement.)

As shown in **Fig. 17**, D_1-TP exhibited two oxidation peak potentials at 1.04 V (17.69 μA) and 1.14 V (13.92 μA). D_2-TP produced stable peaks at 0.79 and 1.10 V, with 22.97 and 12.81 μA currents, respectively (**Fig. 18**). The oxidation peaks of D_3-TP were detected at potentials about 0.76 V and 1.05 V with oxidation currents of 16.11 μA and 4.62 μA, respectively (**Fig. 19**). Given their increased stability and higher values, their initial peaks were selected as the primary oxidation signals for further studies.

The increase in pH resulted in shifts of all oxidation signals, demonstrating the participation of protons in the drug oxidation process, as indicated by changes in peak potentials [115]. The triazolopyrimidinone structure has the potential to undergo tautomerization, resulting in the formation of triazolopyrimidinol through an H-atom shifting process. Various factors influence the stability of the two tautomers, including substitutes, aromatic properties, and hydrogen bonds. The redox mechanism (oxidation and reduction reactions) of Ds-TP on the PGE surface involves the oxidation of the phenol structure within the compound. The heteroatoms in the conjugated amines may affect the potency of oxidation, introducing changes to the overall oxidation properties of the compounds. Considering the tautomerization involving the phenolic form within the heteroaromatic ring and the impact of amine substitution, it is probable that the compound possesses oxidative properties.

4.2. Effect of Concentration

DPV voltammograms for different concentrations of drug candidates were given in Figures 20A, 21A, and 22A, respectively. Also, the response-concentration relationship for each drug candidate has been added, and it is depicted as linear with increasing concentration.

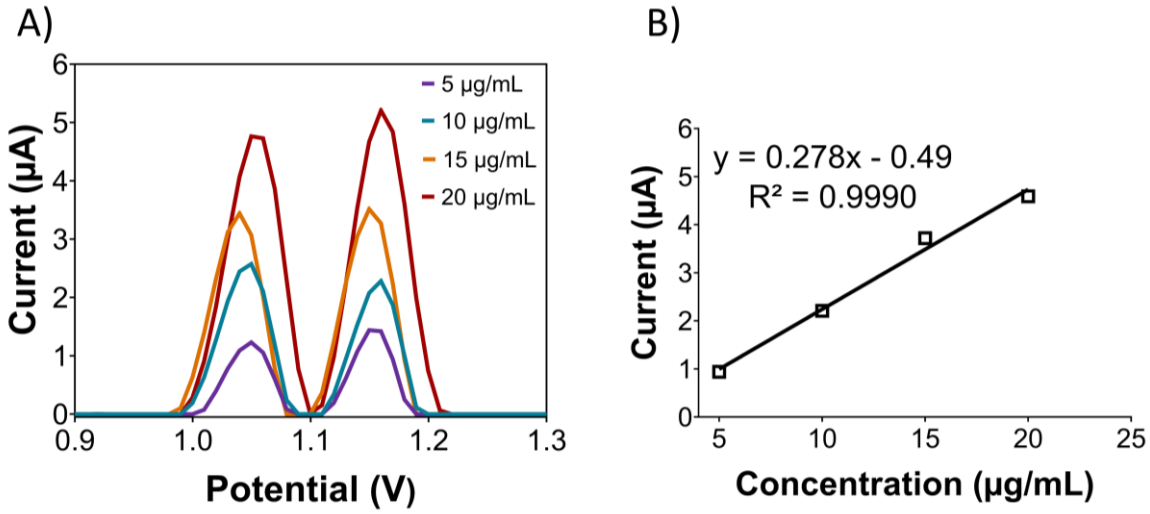


Figure 20. DPV measurements were carried out (scan rate, 100 mV/s) using concentrations ranging from 5 to 20 µg/mL of D_1-TP immobilized on PGE (A). The calibration curve demonstrates the relationship between the first oxidation signal of D_1-TP and its concentration (B).

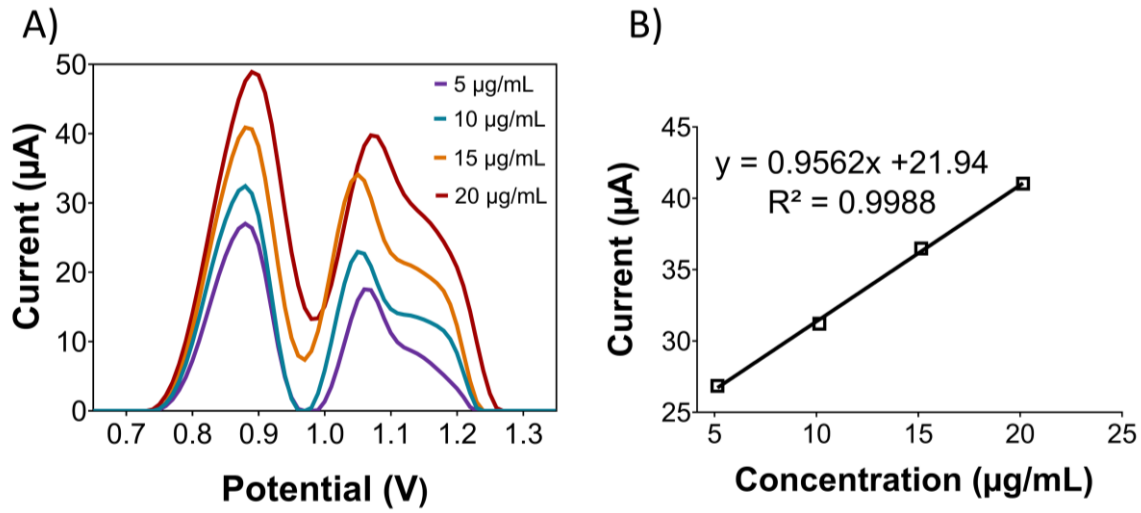


Figure 21. DPV measurements were performed (scan rate, 100 mV/s) using varying concentrations ranging from 5 to 20 µg/mL of D_2-TP immobilized on PGE (A), and the calibration curve was obtained using the first oxidation current of D_2-TP (B).

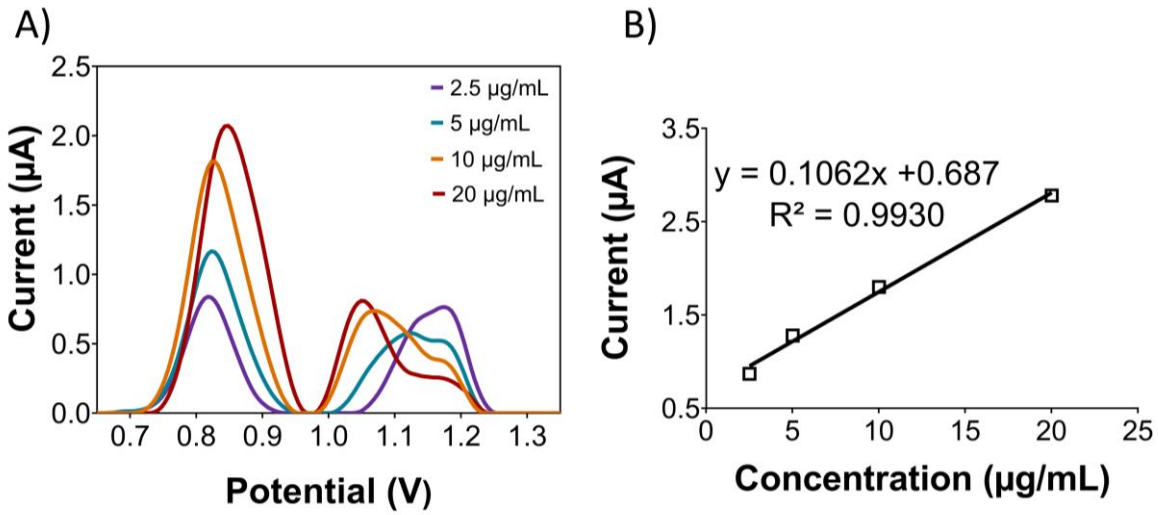


Figure 22. DPV measurements were carried out at (scan rate, 100 mV/s) using varying concentrations of D_3-TP from 2.5 µg/mL to 20 µg/mL (A), and the calibration curve was obtained using the first oxidation current of D_3-TP (B).

According to the calibration plots, LOD was calculated for Ds-TP. LOD for D_1-TP, D_2-TP, and D_3-TP were 1.5, 1.0 and 2.0 µg/mL, respectively.

4.3. Effect of Scan Rate

Scan rate studies were performed to determine the possible reaction mechanisms of drug candidates. CV voltammograms of drug candite molecules at the PGE were recorded for various scan rates between 25 and 150 mV/s. As a result, the current response against the scan rates was linear for each drug candidate.

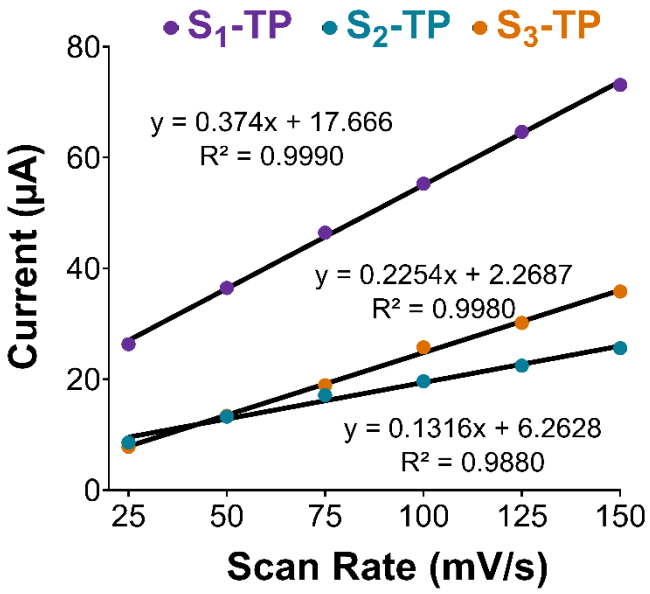


Figure 23. The effect of the scan rate on the peak current was investigated through CV measurements conducted at scan rates ranging from 25 to 150 mV/s.

There is a linear relationship between the peak current (Ip) and scan rate (v) (**Fig. 23**);

D_1-TP; Ip (μA) = 0.374 v + 17.666 (R^2=0.9990) **(3)**

D_2-TP; Ip (μA) = 0.1316 v + 6.2628 (R^2=0.9880) **(4)**

D_3-TP; Ipa(μA) = 0.2254 v + 2.2687 (R^2=0.9980) **(5)**

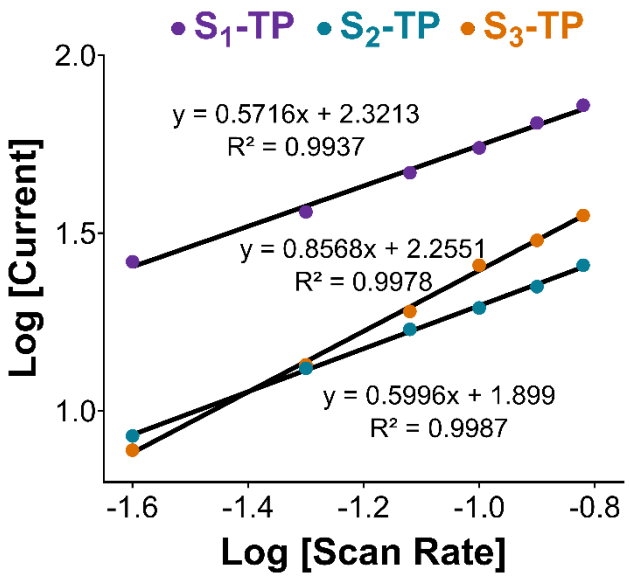


Figure 24. Calibration plot of log scan rate Vs log current of drug candidates.

Linear behaviour is observed between log (Ip) and log (v) (**Fig. 24**);

D_1-TP; $log\ Ip$ = 0.5716$log\ v$ + 2.3213 (R^2=0.9937) **(6)**

D_2-TP; $log\ Ip$ = 0.5996$log\ v$ + 1.899 (R^2=0.9987) **(7)**

D_3-TP; $log\ Ip$ = 0.8568log v + 2.2551 (R^2=0.9978) **(8)**

If the obtained slope is close to 0.5, it suggests the presence of diffusion-controlled reactions. Conversely, slopes approaching the theoretical value of 1 indicate a significant influence of adsorption in the response [116]. The slopes of equations 6 and 7 were found to be 0.57 and 0.60, which suggests that the electrochemical oxidation processes of D_1-TP and D_2-

TP were diffusion-regulated. According to Equation 8, the slope is 0.86, indicating that the electrode process of D_3-TP was controlled by adsorption.

4.4. Stability Results

The stability results of drug candidate molecules are shown in **Fig. 25**. At room temperature (25 ºC), D_1-TP and D_3-TP showed consistent stability during 30 days without significant variations in their current values.

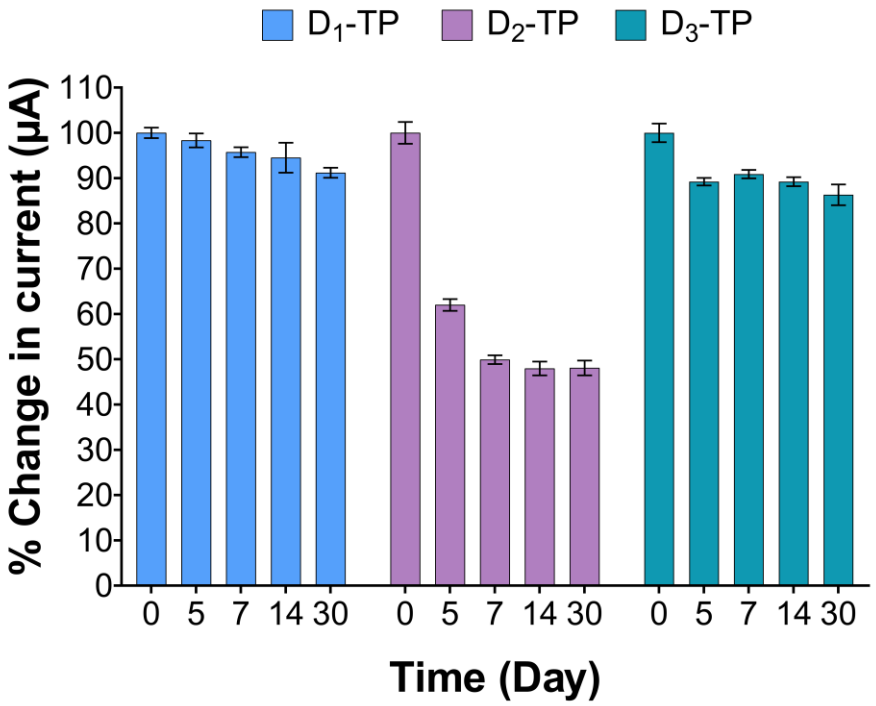


Figure 25. Bar graph expressing the stability of D_1-TP, D_2-TP and D_3-TP investigated under storage conditions by monitoring DPV technique. DPV voltammograms of drug candidates were recorded after preparation, 5 days, 7 days, 14 days and 30 days.

The current percentage for D_1-TP decreased slightly from the first day to 30 days. During the 30 days, there was a decrease of 9.81% in the current value of D_1-TP. From day 0 to day 30, there was a substantial change in the % current of D_2-TP. The current percentage between 7 days and 30 days decreased twice as much as the current percentage at the beginning of the experiment. The current value of D_3-TP experienced a significant decrease to 89.22% on day 5 and further decreased to 86.33% on day 30. As a result, D_1-TP and D_3-TP could be stored in storage conditions (in the dark room and at 25 °C) for long-term use because they retained their pharmaceutical properties.

4.5. Interaction Results

The binding of D_1-TP and D_3-TP to dsDNA bases inhibits the oxidation of dsDNA bases. In contrast, the binding of D_2-TP has enhanced the activity of dsDNA.

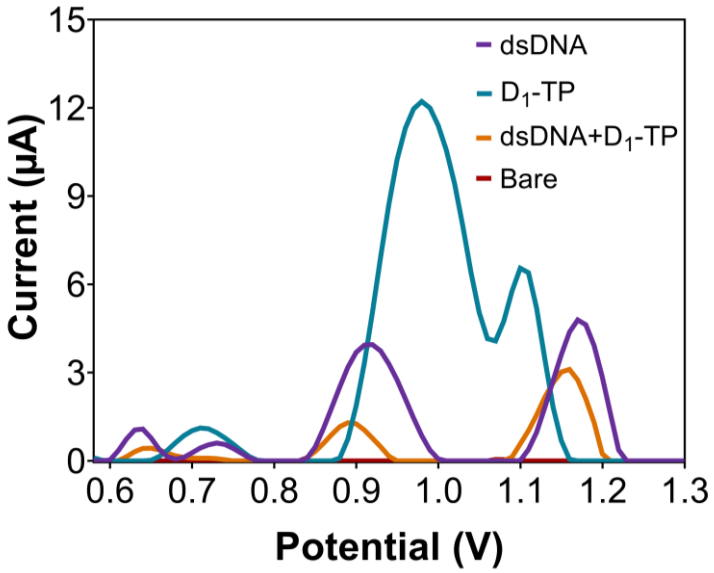


Figure 26. The interaction of D_1-TP with dsDNA. The DPVs were recorded on bare PGE (red), PGE coated with D_1-TP (turquoise), PGE coated with dsDNA (purple), and PGE coated with dsDNA+D_1-TP (orange).

In the absence of D_1-TP, dsDNA exhibits two peaks at 0.92 V as 3.95 µA and 1.17 V as 4.79 µA, respectively **(Fig. 26)**. In the presence of D_1-TP, dsDNA peak potential showed a notable shift towards lower potential values, precisely at 0.89 V and 1.16 V. The dsDNA peak current partially changed and shifted. Peak current values of dsDNA were determined as 1.30 and 3.11 µA, respectively.

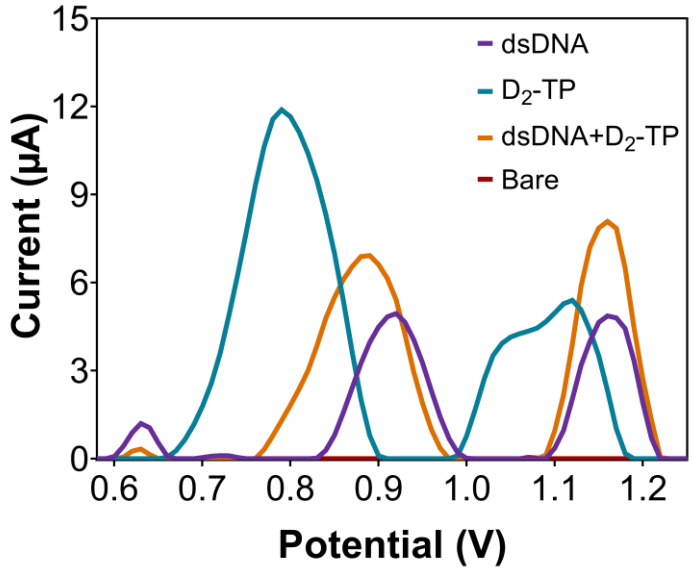


Figure 27. The interaction of D_2-TP with dsDNA. The DPVs were recorded on bare PGE (red), PGE coated with D_2-TP (turquoise), PGE coated with dsDNA (purple), and PGE coated with DNA+D_2-TP (orange).

In the absence of D_2-TP, dsDNA showed the two peaks at 0.92 and 1.16 V, respectively (**Fig. 27)**. Peak currents of dsDNA were 4.94 µA and 4.86 µA. Following the interaction with D_2-TP, a negative shift occurred in the first dsDNA peak potential. There was no change in other peak potential values of dsDNA. After the interaction, dsDNA peak currents were 6.92 µA and 8.08 µA.

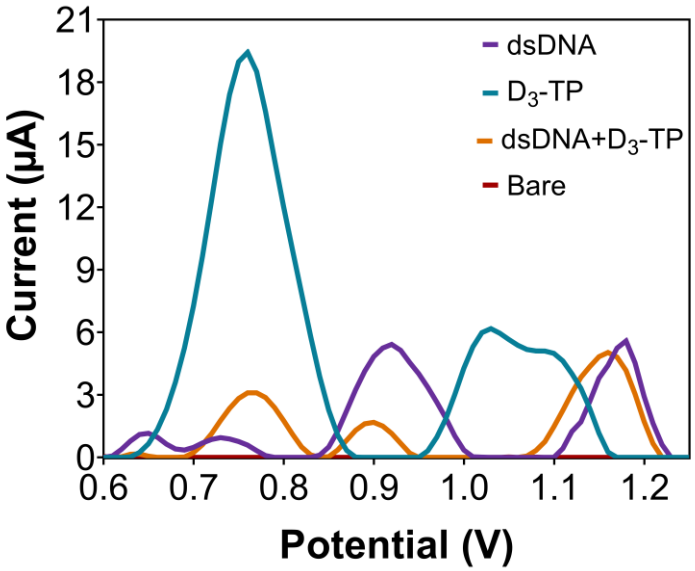


Figure 28. Interaction of D_3-TP–dsDNA. The DPVs were recorded on bare PGE (red), PGE coated with D_3-TP (turquoise), PGE coated with dsDNA (purple), and PGE coated with DNA+D_3-TP (orange).

In **Fig. 28**, the oxidation signals of dsDNA were recorded at 0.92 V and 1.18 V. In the presence of D_3-TP, dsDNA peak potential slightly shifts towards smaller values. The peak current values of dsDNA were initially determined as 5.42 µA and 5.58 µA. After the interaction, dsDNA peak currents were measured as 3.07, 1.66, and 5.03 µA, respectively.

The results showed that dsDNA oxidation potentials decreased after interacting with Ds-TP. The irreversible electrode process may be responsible for the change in peak potential to the negative side. The electrostatic interaction between Ds-TP and dsDNA is responsible for the peak potential shift towards the negative side [117].

4.6. Results of Screen-Printed Electrode (SPE) Experiments

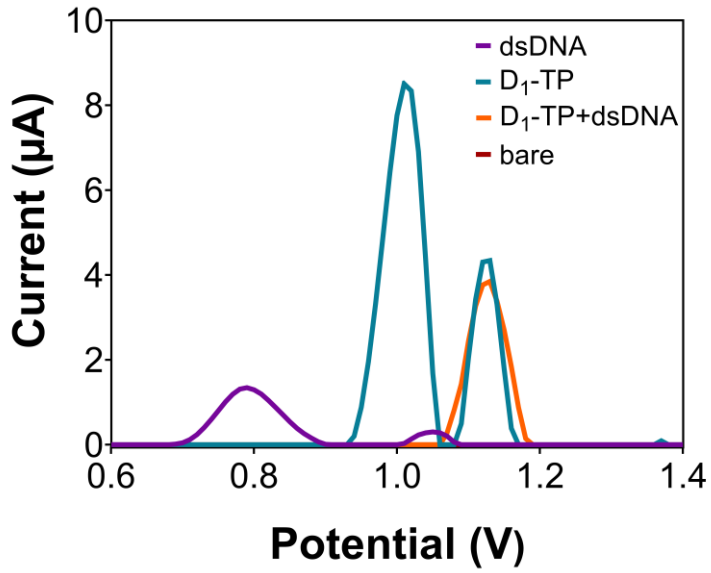


Figure 29. Interaction of D_1-TP–dsDNA. DPV measurements were conducted to analyze the interaction of D_1-TP with dsDNA-modified SPE. DPVs were recorded on different electrodes: bare SPE (red), SPE coated with D_1-TP (turquoise), SPE coated with dsDNA (purple), and SPE coated with DNA+D_1-TP (orange).

In **Fig. 29**, oxidation signals of dsDNA were recorded at 0.79 V as 1.34 µA and 1.05 V as 0.30 µA, respectively. A more positive shoulder appeared after interacting with D_1-TP, as represented by the orange curve at 1.13 V. The peak current value of dsDNA was determined as 3.85 µA.

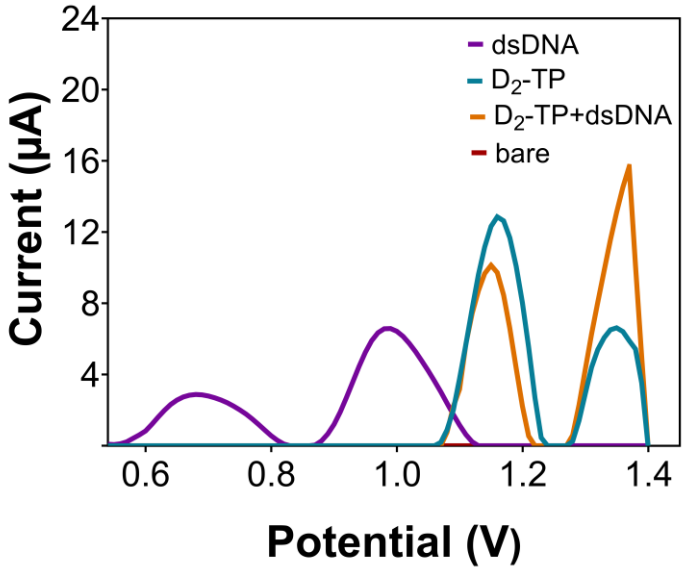


Figure 30. Interaction of D_2-TP–dsDNA. DPV measurements were conducted to analyze the interaction of D_2-TP with dsDNA-modified SPE. DPVs were recorded on different electrodes: bare SPE (red), SPE coated with D_2-TP (turquoise), SPE coated with dsDNA (purple), and SPE coated with DNA+D_2-TP (orange).

In **Fig. 30**, the dsDNA exhibits the oxidation peaks at 0.68 V as 2.88 µA and 0.99 V as 6.59 µA, respectively. After interaction with D_2-TP, dsDNA peak potential shifted towards higher potential values of 1.15 V and 1.37, respectively. The peak current of dsDNA slightly shifted towards a higher value. The peak current value of dsDNA was determined as 10.14 µA and 15.66 µA, respectively.

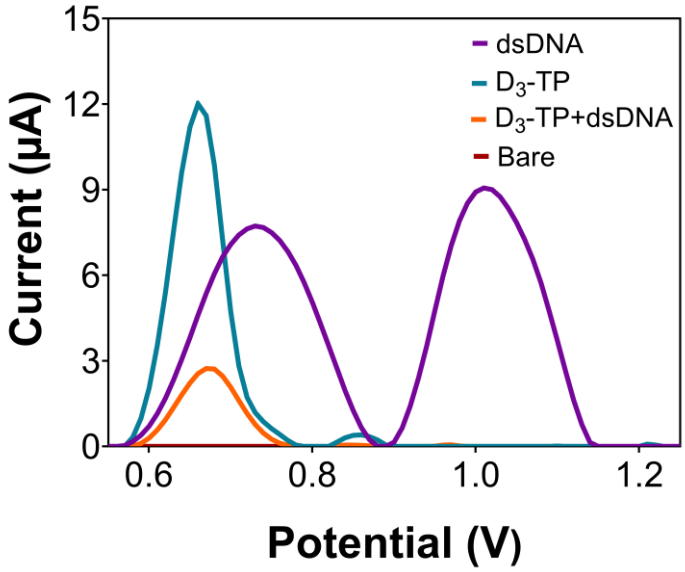


Figure 31. Interaction of D_3-TP–dsDNA. DPV measurements were conducted to analyze the interaction of D_3-TP with dsDNA-modified SPE. DPVs were recorded on different electrodes: bare SPE (red), SPE coated with D_3-TP (turquoise), SPE coated with dsDNA (purple), and SPE coated with DNA+ D_3-TP (orange).

In **Fig. 31**, dsDNA displayed two signals at 0.73 and 1.01 V, respectively. The orange curve indicates the appearance of a more negative shoulder caused by the intercalation of D_3-TP among the base pairs in dsDNA. The value shifted after the interaction was obtained as 0.67 V. In the absence of D_3-TP, peak current values of dsDNA were 7.72 µA and 9.06 µA, respectively. The peak current value of dsDNA was determined as 2.73 µA.

5. DISCUSSIONS

Electrochemical properties and dsDNA binding features of triazolopyrimidinone derivatives (D_1-TP, D_2-TP and D_3-TP) were analyzed with this study, attributed to their purine analog chemical structures. D_1-TP has been introduced to the literature. Additionally, the electrochemical behaviour and its interaction mechanism with dsDNA were studied. Furthermore, this study presented the first comprehensive spectral characterization data of D_2-TP and D_3-TP into the literature (Patent No; WO 2010/056630 A2).

In the initial stage, optimization studies (encompassed pH, concentration and scan rate), stability studies and interaction studies were conducted for triazolopyrimidinone derivatives using pencil graphite electrodes. The pH study resulted in the selection of a pH of 3.8 for the dilution buffer for D_1-TP and D_2-TP and a pH of 5.6 for D_3-TP. Subsequent experiments were then prepared to utilize these specific buffer solutions. Although the drug candidate molecules exhibit stability at pH 3.8 and 5.6, the typical pH of the body ranges from 7.35 to 7.45. However, further investigation is needed, and essential points that should be considered for additional research include this discrepancy, as it may limit conclusive results in studies that progress further.

The analytical concentration ranges of drugs, the LOD for D_1-TP, D_2-TP and D_3-TP, were determined to be 1.5, 1.0 and 2.0 µg/mL. The obtained results highlight the significance of the features of the instruments and methodological optimization studies, in addition to the sensitivity of the analytical approaches used in this study.

For each drug candidate, the current response against the scan rates was linear, according to the scan rate study. D_1-TP and D_2-TP exhibited controlled electrochemical oxidation via diffusion, while D_3-TP exhibited regulated electrochemical oxidation via adsorption.

Following these, stability experiments were conducted. In studies, the efficacy of the drug candidates was assessed. At room temperature (25 ºC), D_1-TP and D_3-TP demonstrated robust stability over a 30-day storage period, with no significant percentage changes in current values. On the other hand, a slight decrease in the D_2-TP percentage of current was noticed from day 0 to day 30. The reason for the relatively lower stability of D_2-TP compared to other candidates may originate from structural differences. Specifically, the oxygen groups in the chemical structure of D_2-TP can impact the reactivity and stability of this molecule. Compared to other candidates, these groups might lead to faster chemical changes or degradation for D_2-TP.

The investigation of DNA-drug interactions was conducted to contribute to the advancement of drug designs. The dsDNA peak potential changed significantly due to the Ds-TP–dsDNA interaction. When dsDNA interacted with D_S-TP, the peak potential of dsDNA shifted negatively.

The binding of D_1-TP and D_3-TP to dsDNA inhibits the oxidation signal of dsDNA bases. Conversely, the interaction of D_2-TP with dsDNA has enhanced the activity of dsDNA. The dsDNA peak potential change towards more negative values indicates an electrostatic mode underlying the DNA-drug interaction mechanism. Understanding such an interaction mechanism provides valuable insights into the nature of DNA-drug interactions and can guide further exploration of their binding characteristics. Electrostatic interactions play a significant role in characterizing molecular interactions as they involve charge interactions at the molecular level.

After optimization studies based on PGE, the effect of drug candidates on dsDNA was subsequently investigated using an SPE. This exploration was carried out to facilitate the integration of these drug candidates with dsDNA into an electrochemical biosensor system. Utilizing a three-electrode system in electrochemical analyses presents challenges related to precise integration and potential electrode movement, resulting in errors and user-dependent variability. To overcome these challenges, a screen-printed electrode was chosen for its user-

friendly and space-efficient design, promoting repeatability and ensuring consistent results in the electrochemical biosensor platform.

A more positive shoulder appeared after the D_1-TP interaction between dsDNA in SPE experiments. Conversely, the peak current of dsDNA noticed a slight shift towards a higher value after the D_2-TP interaction. After the interaction of D_3-TP between dsDNA, a more negative shoulder appeared.

The differences between these two experiments (PGE-based and SPE-based) could stem from various factors, including the electrode designs and, notably, the materials used to produce electrodes. Carbon is used for the working and auxiliary electrodes in the SPE, whereas silver is used for the reference electrode. PGE is predominantly carbon material and characterized by a simple structure, making it a widely used electrode. On the other hand, SPE is produced using a specific printing technique, providing more design flexibility to create a specialized sensor platform. Advantages of SPE include better repeatability and ease of use. However, the characteristics of both electrode types can influence measurement results. For instance, surface materials and electrode design can create variations in determining DNA-drug interactions and recording the electrochemical signals of these interactions.

6. CONCLUSION AND FUTURE DIRECTIONS

DNA is a widely targeted drug component due to its pivotal role in various disease processes. Exploring the interactions between drugs and DNA is crucial for gaining valuable insights into the mechanisms of drug action, thereby facilitating the development of novel targeted drugs. From this perspective, examining drug-DNA reactions is essential in pharmaceutical studies. In this study, complete spectral characterization data and Ds-TP interaction with dsDNA were studied for the first time in the literature by DPV and CV. The electrochemical behaviour of dsDNA changed when bound to the Ds-TP. These results demonstrate the requirement to consider the direct interaction between D_S-TP and DNA when evaluating the mechanism behind the noticeable biological effects of the drugs.

SPEs provide an easy-to-use and sensitive detection approach for investigating the interaction mechanisms between dsDNA and drugs in electroanalytical chemistry. With the adaptation of the SPE to the biosensor system, a simple and portable biosensor platform was produced. This biosensor operates on the principle of binding between Ds-TP and dsDNA. This

biosensor offers users an easy testing opportunity with a user-friendly GUI. For further studies, the developed biosensor can be tested with actual samples, and its sensitivity can be enhanced by coating the sensor surface with various substances, for example, carbon nanotubes, gold nanoparticles, etc.

7. REFERENCES

[1] K. De la Cruz Morales, G. Alarcón-Angeles, and A. Merkoçi, "Nanomaterial-based Sensors for the Study of DNA Interaction with Drugs," *Electroanalysis*, vol. 31, no. 10, pp. 1845–1867, Oct. 2019, doi: 10.1002/elan.201900286.

[2] K. Morawska, T. Popławski, W. Ciesielski, and S. Smarzewska, "Electrochemical and spectroscopic studies of the interaction of antiviral drug Tenofovir with single and double stranded DNA," *Bioelectrochemistry*, vol. 123, pp. 227–232, Oct. 2018, doi: 10.1016/j.bioelechem.2018.06.002.

[3] M. Sirajuddin, S. Ali, and A. Badshah, "Drug–DNA interactions and their study by UV–Visible, fluorescence spectroscopies and cyclic voltametry," *J. Photochem. Photobiol. B Biol.*, vol. 124, pp. 1–19, Jul. 2013, doi: 10.1016/j.jphotobiol.2013.03.013.

[4] B. Montaner *et al.*, "DNA Interaction and Dual Topoisomerase I and II Inhibition Properties of the Anti-Tumor Drug Prodigiosin," *Toxicol. Sci.*, vol. 85, no. 2, pp. 870–879, Jun. 2005, doi: 10.1093/toxsci/kfi149.

[5] A. Romdhane, A. Ben Said, M. Cherif, and H. Ben Jannet, "Design, synthesis and anti-acetylcholinesterase evaluation of some new pyrazolo[4,3-e]-1,2,4-triazolo[1,5-c]pyrimidine derivatives," *Med. Chem. Res.*, vol. 25, no. 7, pp. 1358–1368, Jul. 2016, doi: 10.1007/s00044-016-1576-0.

[6] N. Shah, M. B. Arain, and M. Soylak, "Historical background: milestones in the field of development of analytical instrumentation," in *New Generation Green Solvents for Separation and Preconcentration of Organic and Inorganic Species*, Elsevier, 2020, pp. 45–73.

[7] K. Robards, P. R. Haddad, and P. E. Jackson, "High-performance Liquid Chromatography—Instrumentation and Techniques," in *Principles and Practice of Modern Chromatographic Methods*, Elsevier, 2004, pp. 227–303.

[8] N. Elgrishi, K. J. Rountree, B. D. McCarthy, E. S. Rountree, T. T. Eisenhart, and J. L. Dempsey, "A Practical Beginner's Guide to Cyclic Voltammetry," *J. Chem. Educ.*, vol. 95, no. 2, pp. 197–206, Feb. 2018, doi: 10.1021/acs.jchemed.7b00361.

[9] P. T. Kissinger and W. R. Heineman, "Cyclic voltammetry," *J. Chem. Educ.*, vol. 60, no. 9, p. 702, Sep. 1983, doi: 10.1021/ed060p702.

[10] N. K. Bakirhan, B. Uslu, and S. A. Ozkan, "Sensitive and Selective Assay of Antimicrobials on Nanostructured Materials by Electrochemical Techniques," in *Nanostructures for Antimicrobial Therapy*, Elsevier, 2017, pp. 55–83.

[11] D. H. Evans, K. M. O'Connell, R. A. Petersen, and M. J. Kelly, "Cyclic voltammetry," *J. Chem. Educ.*, vol. 60, no. 4, p. 290, Apr. 1983, doi: 10.1021/ed060p290.

[12] M. Smyth, "Cyclic voltammetry," *TrAC Trends Anal. Chem.*, vol. 13, no. 8, p. 341, Sep. 1994, doi: 10.1016/0165-9936(94)87010-1.

[13] J. Liu, Y. Xu, S. Liu, S. Yu, Z. Yu, and S. S. Low, "Application and Progress of Chemometrics in Voltammetric Biosensing," *Biosensors*, vol. 12, no. 7, p. 494, Jul. 2022, doi: 10.3390/bios12070494.

[14] B. J. Venton and D. J. DiScenza, “Voltammetry,” in *Electrochemistry for Bioanalysis*, Elsevier, 2020, pp. 27–50.

[15] F. R. Simões and M. G. Xavier, “Electrochemical Sensors,” in *Nanoscience and its Applications*, Elsevier, 2017, pp. 155–178.

[16] M. A. Deshmukh *et al.*, “EDTA-modified PANI/SWNTs nanocomposite for differential pulse voltammetry based determination of Cu(II) ions,” *Sensors Actuators B Chem.*, vol. 260, pp. 331–338, May 2018, doi: 10.1016/j.snb.2017.12.160.

[17] V. Mirceski, R. Gulaboski, M. Lovric, I. Bogeski, R. Kappl, and M. Hoth, “Square-Wave Voltammetry: A Review on the Recent Progress,” *Electroanalysis*, vol. 25, no. 11, pp. 2411–2422, Nov. 2013, doi: 10.1002/elan.201300369.

[18] R. Gulaboski, V. Mirčeski, I. Bogeski, and M. Hoth, “Protein film voltammetry: electrochemical enzymatic spectroscopy. A review on recent progress,” *J. Solid State Electrochem.*, vol. 16, no. 7, pp. 2315–2328, Jul. 2012, doi: 10.1007/s10008-011-1397-5.

[19] N. Mohamad Nor, N. S. Ridhuan, and K. Abdul Razak, “Progress of Enzymatic and Non-Enzymatic Electrochemical Glucose Biosensor Based on Nanomaterial-Modified Electrode,” *Biosensors*, vol. 12, no. 12, p. 1136, Dec. 2022, doi: 10.3390/bios12121136.

[20] S. Girousi and Z. Stanic, “The Last Decade of Carbon Paste Electrodes in DNA Electrochemistry,” *Curr. Anal. Chem.*, vol. 7, no. 1, pp. 80–100, Jan. 2011, doi: 10.2174/157341111793797608.

[21] B. Goswami and D. Mahanta, “Fe 3 O 4 -Polyaniline Nanocomposite for Non-enzymatic Electrochemical Detection of 2,4-Dichlorophenoxyacetic Acid,” *ACS Omega*, vol. 6, no. 27, pp. 17239–17246, Jul. 2021, doi: 10.1021/acsomega.1c00983.

[22] H. T. Purushothama and Y. Arthoba Nayaka, “Pencil graphite electrode based electrochemical system for the investigation of antihypertensive drug hydrochlorothiazide: An electrochemical study,” *Chem. Phys. Lett.*, vol. 734, p. 136718, Nov. 2019, doi: 10.1016/j.cplett.2019.136718.

[23] S. Ahmadi, H. Fini, T. Ho, P. J. Nadoushan, H.-B. Kraatz, and K. Kerman, “Development of an Electrochemical Sensor Using Pencil Graphite Electrode for Monitoring UV-Induced DNA Damage,” *J. Chem. Educ.*, vol. 97, no. 12, pp. 4445–4452, Dec. 2020, doi: 10.1021/acs.jchemed.9b01065.

[24] I. G. David, D.-E. Popa, and M. Buleandra, “Pencil Graphite Electrodes: A Versatile Tool in Electroanalysis,” *J. Anal. Methods Chem.*, vol. 2017, pp. 1–22, 2017, doi: 10.1155/2017/1905968.

[25] S. Antherjanam and B. Saraswathyamma, “Simultaneous electrochemical determination of hydrazine and hydroxylamine on a thiadiazole derivative modified pencil graphite electrode,” *Mater. Chem. Phys.*, vol. 275, p. 125223, Jan. 2022, doi: 10.1016/j.matchemphys.2021.125223.

[26] S. Šafranko *et al.*, “Electroactivated Disposable Pencil Graphite Electrode – New, Cost-effective, and Sensitive Electrochemical Detection of Bioflavonoid Hesperidin,” *Electroanalysis*, vol. 33, no. 4, pp. 1063–1071, Apr. 2021, doi: 10.1002/elan.202060511.

[27] E. Mirmomtaz, A. A. Ensafi, and S. Soleimanian-Zad, “Determination of amiloride using a ds-DNA-modified pencil graphite electrode based on guanine and adenine signals,” *Electrochim. Acta*, vol. 54, no. 3, pp. 1141–1146, Jan. 2009, doi: 10.1016/j.electacta.2008.09.003.

[28] M. W. Shinwari, D. Zhitomirsky, I. A. Deen, P. R. Selvaganapathy, M. J. Deen, and D. Landheer, “Microfabricated Reference Electrodes and their Biosensing Applications,” *Sensors*, vol. 10, no. 3, pp. 1679–1715, Mar. 2010, doi: 10.3390/s100301679.

[29] M.-H. Yun, J.-W. Yeon, J. Hwang, C. S. Hong, and K. Song, “A calibration technique for an Ag/AgCl reference electrode utilizing the relationship between the electrical conductivity and the KCl concentration of the internal electrolyte,” *J. Appl. Electrochem.*, vol. 39, no. 12, pp. 2587–2592, Dec. 2009, doi: 10.1007/s10800-009-9955-6.

[30] M. Sophocleous and J. K. Atkinson, “A review of screen-printed silver/silver chloride (Ag/AgCl) reference electrodes potentially suitable for environmental potentiometric sensors,” *Sensors Actuators A Phys.*, vol. 267, pp. 106–120, Nov. 2017, doi: 10.1016/j.sna.2017.10.013.

[31] J. Roscher and R. Holze, “Reference Electrodes,” *Encyclopedia*, vol. 3, no. 2, pp. 478–489, Apr. 2023, doi: 10.3390/encyclopedia3020033.

[32] G. Jerkiewicz, “Applicability of Platinum as a Counter-Electrode Material in Electrocatalysis Research,” *ACS Catal.*, vol. 12, no. 4, pp. 2661–2670, Feb. 2022, doi: 10.1021/acscatal.1c06040.

[33] N.-B. Mincu, V. Lazar, D. Stan, C. M. Mihailescu, R. Iosub, and A. L. Mateescu, “Screen-Printed Electrodes (SPE) for In Vitro Diagnostic Purpose,” *Diagnostics*, vol. 10, no. 8, p. 517, Jul. 2020, doi: 10.3390/diagnostics10080517.

[34] R. Pol, F. Céspedes, D. Gabriel, and M. Baeza, “Fully integrated screen-printed sulfide-selective sensor on a 3D-printed potentiometric microfluidic platform,” *Sensors Actuators B Chem.*, vol. 290, pp. 364–370, Jul. 2019, doi: 10.1016/j.snb.2019.03.132.

[35] J. Puy-Llovera, C. Pérez-Ràfols, N. Serrano, J. M. Díaz-Cruz, C. Ariño, and M. Esteban, “Selenocystine modified screen-printed electrode as an alternative sensor for the voltammetric determination of metal ions,” *Talanta*, vol. 175, pp. 501–506, Dec. 2017, doi: 10.1016/j.talanta.2017.07.089.

[36] K. Ri, S. Kim, H. Paek, C. Hong, and M. Jon, “Determination of sulfide at screen-printed electrode modified with ferricyanide-doped partially quaternized poly (4-vinylpyridine),” *J. Electroanal. Chem.*, vol. 853, p. 113540, Nov. 2019, doi: 10.1016/j.jelechem.2019.113540.

[37] A. K. M. S. Inam, M. A. C. Angeli, A. Douaki, B. Shkodra, P. Lugli, and L. Petti, “An Aptasensor Based on a Flexible Screen-Printed Silver Electrode for the Rapid Detection of Chlorpyrifos,” *Sensors*, vol. 22, no. 7, p. 2754, Apr. 2022, doi: 10.3390/s22072754.

[38] M. Elhachem, E. Bou-Maroun, M. Abboud, R. G. Maroun, and P. Cayot, “Combination of Screen-Printed Carbon Electrode and Molecularly Imprinted Polymers for the Selective Determination of Phenolic Compounds in Wine,” *Antioxidants*, vol. 11, no. 10, p. 2036, Oct. 2022, doi: 10.3390/antiox11102036.

[39] S. Chen *et al.*, “Microfluidic Device Directly Fabricated on Screen-Printed Electrodes for Ultrasensitive Electrochemical Sensing of PSA,” *Nanoscale Res. Lett.*, vol. 14, no. 1, p. 71, Dec. 2019, doi: 10.1186/s11671-019-2857-6.

[40] M. Dı, M. Zaguirre, and C. Arin, “Screen-printed Electrodes for the Determination of Iridium in Drugs,” pp. 2925–2930, 2018, doi: 10.1002/elan.201800502.

[41] A. Haleem, M. Javaid, R. P. Singh, R. Suman, and S. Rab, “Biosensors applications in medical field: A brief review,” *Sensors Int.*, vol. 2, p. 100100, 2021, doi: 10.1016/j.sintl.2021.100100.

[42] M. Song *et al.*, “Materials and Methods of Biosensor Interfaces With Stability,” *Front. Mater.*, vol. 7, Jan. 2021, doi: 10.3389/fmats.2020.583739.

[43] F. Narita *et al.*, “A Review of Piezoelectric and Magnetostrictive Biosensor Materials for Detection of COVID-19 and Other Viruses,” *Adv. Mater.*, vol. 33, no. 1, Jan. 2021, doi: 10.1002/adma.202005448.

[44] Y. Yim, H. Shin, S. M. Ahn, and D.-H. Min, “Graphene oxide-based fluorescent biosensors and their biomedical applications in diagnosis and drug discovery,” *Chem. Commun.*, vol. 57, no. 77, pp. 9820–9833, 2021, doi: 10.1039/D1CC02157E.

[45] M. Y. Chin *et al.*, “Genetically Encoded, pH-Sensitive mTFP1 Biosensor for Probing Lysosomal pH,” *ACS Sensors*, vol. 6, no. 6, pp. 2168–2180, Jun. 2021, doi: 10.1021/acssensors.0c02318.

[46] E. Cesewski and B. N. Johnson, “Electrochemical biosensors for pathogen detection,” *Biosens. Bioelectron.*, vol. 159, p. 112214, Jul. 2020, doi: 10.1016/j.bios.2020.112214.

[47] A. Balaji and J. Zhang, “Electrochemical and optical biosensors for early-stage cancer diagnosis by using graphene and graphene oxide,” *Cancer Nanotechnol.*, vol. 8, no. 1, p. 10, Dec. 2017, doi: 10.1186/s12645-017-0035-z.

[48] J. Liu *et al.*, “Salivary Cortisol Determination on Smartphone-Based Differential Pulse Voltammetry System,” *Sensors*, vol. 20, no. 5, p. 1422, Mar. 2020, doi: 10.3390/s20051422.

[49] C. Griesche and A. J. Baeumner, “Biosensors to support sustainable agriculture and food safety,” *TrAC Trends Anal. Chem.*, vol. 128, p. 115906, Jul. 2020, doi: 10.1016/j.trac.2020.115906.

[50] M. Mahmoudpour, J. Ezzati Nazhad Dolatabadi, M. Torbati, and A. Homayouni-Rad, “Nanomaterials based surface plasmon resonance signal enhancement for detection of environmental pollutions,” *Biosens. Bioelectron.*, vol. 127, pp. 72–84, Feb. 2019, doi: 10.1016/j.bios.2018.12.023.

[51] W. K. Abdelbasset *et al.*, “Comparison and evaluation of the performance of graphene-based biosensors,” *Carbon Lett.*, vol. 32, no. 4, pp. 927–951, Jun. 2022, doi: 10.1007/s42823-022-00338-6.

[52] V. Perumal and U. Hashim, “Advances in biosensors: Principle, architecture and applications,” *J. Appl. Biomed.*, vol. 12, no. 1, pp. 1–15, Jan. 2014, doi: 10.1016/j.jab.2013.02.001.

[53] V. Naresh and N. Lee, “A Review on Biosensors and Recent Development of Nanostructured Materials-Enabled Biosensors,” *Sensors*, vol. 21, no. 4, p. 1109, Feb. 2021, doi: 10.3390/s21041109.

[54] M. Hegde, P. Pai, M. G. Shetty, and K. S. Babitha, “Gold nanoparticle based biosensors for rapid pathogen detection: A review,” *Environ. Nanotechnology, Monit. Manag.*, vol. 18, p. 100756, Dec. 2022, doi: 10.1016/j.enmm.2022.100756.

[55] S. Malik *et al.*, “Nanomaterials-based biosensor and their applications: A review,” *Heliyon*, vol. 9, no. 9, p. e19929, Sep. 2023, doi: 10.1016/j.heliyon.2023.e19929.

[56] G. Luka, S. Ahmad, N. Falcone, and H.-B. Kraatz, “Advances in enzyme-based electrochemical sensors: current trends, benefits, and constraints,” in *Bioelectronics and Medical Devices*, Elsevier, 2019, pp. 555–590.

[57] L. C. Clark and C. Lyons, “ELECTRODE SYSTEMS FOR CONTINUOUS MONITORING IN CARDIOVASCULAR SURGERY,” *Ann. N. Y. Acad. Sci.*, vol. 102, no. 1, pp. 29–45, Oct. 1962, doi: 10.1111/j.1749-6632.1962.tb13623.x.

[58] R. Jain, S. Miri, V. L. Pachapur, and S. K. Brar, “Advances in antibody-based biosensors in environmental monitoring,” in *Tools, Techniques and Protocols for Monitoring Environmental Contaminants*, Elsevier, 2019, pp. 285–305.

[59] B. V. Ayyar and S. Arora, “Antibody-Based Biosensors for Detection of Veterinary Viral Pathogens,” *Adv. Anim. Vet. Sci.*, no. December, 2013, [Online]. Available: http://nexusacademicpublishers.com/table_contents_detail/4/144/html.

[60] G. Caluori *et al.*, “Non-invasive electromechanical cell-based biosensors for improved investigation of 3D cardiac models,” *Biosens. Bioelectron.*, vol. 124–125, pp. 129–135, Jan. 2019, doi: 10.1016/j.bios.2018.10.021.

[61] M. Son and T. H. Park, “The bioelectronic nose and tongue using olfactory and taste receptors: Analytical tools for food quality and safety assessment,” *Biotechnol. Adv.*, vol. 36, no. 2, pp. 371–379, Mar. 2018, doi: 10.1016/j.biotechadv.2017.12.017.

[62] Q. Liu, C. Wu, H. Cai, N. Hu, J. Zhou, and P. Wang, “Cell-Based Biosensors and Their Application in Biomedicine,” *Chem. Rev.*, vol. 114, no. 12, pp. 6423–6461, Jun. 2014, doi: 10.1021/cr2003129.

[63] G. Pasternak, J. Greenman, and I. Ieropoulos, “Self-powered, autonomous Biological Oxygen Demand biosensor for online water quality monitoring,” *Sensors Actuators B Chem.*, vol. 244, pp. 815–822, Jun. 2017, doi: 10.1016/j.snb.2017.01.019.

[64] A. K. Singh, S. Mittal, M. Das, A. Saharia, and M. Tiwari, “Optical biosensors: a decade in review,” *Alexandria Eng. J.*, vol. 67, pp. 673–691, Mar. 2023, doi: 10.1016/j.aej.2022.12.040.

[65] P. Damborský, J. Švitel, and J. Katrlík, “Optical biosensors,” *Essays Biochem.*, vol. 60, no. 1, pp. 91–100, Jun. 2016, doi: 10.1042/EBC20150010.

[66] Y. Chen, J. Liu, Z. Yang, J. S. Wilkinson, and X. Zhou, “Optical biosensors based on refractometric sensing schemes: A review,” *Biosens. Bioelectron.*, vol. 144, p. 111693, Nov. 2019, doi: 10.1016/j.bios.2019.111693.

[67] P. Xiao, S. Sang, Q. Zhang, Y. Ge, Y. Cheng, and D. Zhao, "A membrane-type mechanical biosensor based on magnetic, surface stress and electric coupling enhancement for HSA detection," *Biochem. Eng. J.*, vol. 180, p. 108361, Mar. 2022, doi: 10.1016/j.bej.2022.108361.

[68] P. Lu *et al.*, "Regulatory-sequence mechanical biosensor: A versatile platform for investigation of G-quadruplex/label-free protein interactions and tunable protein detection," *Anal. Chim. Acta*, vol. 1045, pp. 1–9, Jan. 2019, doi: 10.1016/j.aca.2018.09.019.

[69] J. L. Arlett, E. B. Myers, and M. L. Roukes, "Comparative advantages of mechanical biosensors," *Nat. Nanotechnol.*, vol. 6, no. 4, pp. 203–215, Apr. 2011, doi: 10.1038/nnano.2011.44.

[70] S. D. Alharthi, D. Bijukumar, S. Prasad, A. M. Khan, and M. T. Mathew, "Evolution in Biosensors for Cancers Biomarkers Detection: A Review," *J. Bio- Tribo-Corrosion*, vol. 7, no. 2, p. 42, Jun. 2021, doi: 10.1007/s40735-020-00463-7.

[71] D. Martín-Yerga and A. Costa-García, "Towards a blocking-free electrochemical immunosensing strategy for anti-transglutaminase antibodies using screen-printed electrodes," *Bioelectrochemistry*, vol. 105, pp. 88–94, Oct. 2015, doi: 10.1016/j.bioelechem.2015.05.014.

[72] A. K. M. S. Inam *et al.*, "Flexible Screen-Printed Electrochemical Sensors Functionalized with Electrodeposited Copper for Nitrate Detection in Water," *ACS Omega*, vol. 6, no. 49, pp. 33523–33532, Dec. 2021, doi: 10.1021/acsomega.1c04296.

[73] J. Dou, A. Ding, L. Cheng, R. Sekar, H. Wang, and S. Li, "A screen-printed, amperometric biosensor for the determination of organophosphorus pesticides in water samples," *J. Environ. Sci.*, vol. 24, no. 5, pp. 956–962, May 2012, doi: 10.1016/S1001-0742(11)60864-4.

[74] D. Wang *et al.*, "Efficient separation and quantitative detection of Listeria monocytogenes based on screen-printed interdigitated electrode, urease and magnetic nanoparticles," *Food Control*, vol. 73, pp. 555–561, Mar. 2017, doi: 10.1016/j.foodcont.2016.09.003.

[75] H. Mahmoudi-Moghaddam, S. Tajik, and H. Beitollahi, "Highly sensitive electrochemical sensor based on La3+-doped Co3O4 nanocubes for determination of sudan I content in food samples," *Food Chem.*, vol. 286, pp. 191–196, Jul. 2019, doi: 10.1016/j.foodchem.2019.01.143.

[76] A.-E. Radi, A. Khafagy, A. El-shobaky, and H. El-mezayen, "Anodic Voltammetric determination of gemifloxacin using screen-printed carbon electrode," *J. Pharm. Anal.*, vol. 3, no. 2, pp. 132–136, Apr. 2013, doi: 10.1016/j.jpha.2012.10.005.

[77] I. R. Suhito, K.-M. Koo, and T.-H. Kim, "Recent Advances in Electrochemical Sensors for the Detection of Biomolecules and Whole Cells," *Biomedicines*, vol. 9, no. 1, p. 15, Dec. 2020, doi: 10.3390/biomedicines9010015.

[78] R. E. Madrid, F. Ashur Ramallo, D. E. Barraza, and R. E. Chaile, "Smartphone-Based Biosensor Devices for Healthcare: Technologies, Trends, and Adoption by End-Users," *Bioengineering*, vol. 9, no. 3, p. 101, Mar. 2022, doi: 10.3390/bioengineering9030101.

[79] D. Zhang and Q. Liu, “Biosensors and bioelectronics on smartphone for portable biochemical detection,” *Biosens. Bioelectron.*, vol. 75, pp. 273–284, Jan. 2016, doi: 10.1016/j.bios.2015.08.037.

[80] I. Campelo and A. M. Oliveira-brett, “Human Cytochrome P450 (CYP1A2) -dsDNA Interaction in situ Evaluation Using a dsDNA-electrochemical Biosensor,” pp. 1674–1682, 2017, doi: 10.1002/elan.201600713.

[81] N. Sohrabi, A. Valizadeh, S. M. Farkhani, and A. Akbarzadeh, “Basics of DNA biosensors and cancer diagnosis Basics of DNA biosensors and cancer diagnosis,” *Artif. Cells, Nanomedicine, Biotechnol.*, no. November, pp. 1–10, 2014, doi: 10.3109/21691401.2014.976707.

[82] A. M. Oliveira-Brett, J. A. P. Piedade, L. A. Silva, and V. C. Diculescu, “Voltammetric determination of all DNA nucleotides,” *Anal. Biochem.*, vol. 332, no. 2, pp. 321–329, Sep. 2004, doi: 10.1016/j.ab.2004.06.021.

[83] E. Paleček, M. Fojta, F. Jelen, and V. Vetterl, “Electrochemical Analysis of Nucleic Acids,” in *Encyclopedia of Electrochemistry*, Wiley, 2002.

[84] P. Martinkova, A. Kostelnik, T. Valek, and M. Pohanka, “>Main streams in the Construction of Biosensors and Their Applications,” *Int. J. Electrochem. Sci.*, vol. 12, no. 8, pp. 7386–7403, Aug. 2017, doi: 10.20964/2017.08.02.

[85] H. H. Nguyen and M. Kim, “An Overview of Techniques in Enzyme Immobilization,” *Appl. Sci. Converg. Technol.*, vol. 26, no. 6, pp. 157–163, Nov. 2017, doi: 10.5757/ASCT.2017.26.6.157.

[86] V. Sanko and F. Kuralay, “Label-Free Electrochemical Biosensor Platforms for Cancer Diagnosis: Recent Achievements and Challenges,” *Biosensors*, vol. 13, no. 3, p. 333, Mar. 2023, doi: 10.3390/bios13030333.

[87] M. M. Shanbhag, G. Manasa, R. J. Mascarenhas, K. Mondal, and N. P. Shetti, “Fundamentals of bio-electrochemical sensing,” *Chem. Eng. J. Adv.*, vol. 16, p. 100516, Nov. 2023, doi: 10.1016/j.ceja.2023.100516.

[88] S. D. Wijayanti, L. Tsvik, and D. Haltrich, “Recent Advances in Electrochemical Enzyme-Based Biosensors for Food and Beverage Analysis,” *Foods*, vol. 12, no. 18, p. 3355, Sep. 2023, doi: 10.3390/foods12183355.

[89] A. A. Homaei, R. Sariri, F. Vianello, and R. Stevanato, “Enzyme immobilization: an update,” *J. Chem. Biol.*, vol. 6, no. 4, pp. 185–205, Oct. 2013, doi: 10.1007/s12154-013-0102-9.

[90] A.-M. Chiorcea Paquim, T. S. Oretskaya, and A. M. Oliveira Brett, “Adsorption of synthetic homo- and hetero-oligodeoxynucleotides onto highly oriented pyrolytic graphite: Atomic force microscopy characterization,” *Biophys. Chem.*, vol. 121, no. 2, pp. 131–141, May 2006, doi: 10.1016/j.bpc.2005.12.017.

[91] “No Title.” https://www.genome.gov/genetics-glossary/Deoxyribonucleic-.

[92] S. Hmoud Alotaibi and A. Abdalla Momen, “Anticancer Drugs’ Deoxyribonucleic Acid (DNA) Interactions,” in *Biophysical Chemistry - Advance Applications*, IntechOpen, 2020.

[93] D. G. Díaz-Gómez, R. Galindo-Murillo, and F. Cortés-Guzmán, "The Role of the DNA Backbone in Minor-Groove Ligand Binding," *ChemPhysChem*, vol. 18, no. 14, pp. 1909–1915, Jul. 2017, doi: 10.1002/cphc.201700260.

[94] A.-M. Chiorcea-Paquim and A. M. Oliveira-Brett, "DNA Electrochemical Biosensors for In Situ Probing of Pharmaceutical Drug Oxidative DNA Damage," *Sensors*, vol. 21, no. 4, p. 1125, Feb. 2021, doi: 10.3390/s21041125.

[95] G. Magdy, M. A. Shaldam, F. Belal, and H. Elmansi, "Multi-spectroscopic, thermodynamic, and molecular docking/dynamic approaches for characterization of the binding interaction between calf thymus DNA and palbociclib," *Sci. Rep.*, vol. 12, no. 1, p. 14723, Aug. 2022, doi: 10.1038/s41598-022-19015-9.

[96] R. Nimal *et al.*, "Development of the electrochemical, spectroscopic and molecular docking approaches toward the investigation of interaction between DNA and anti-leukemic drug azacytidine," *Bioelectrochemistry*, vol. 146, p. 108135, Aug. 2022, doi: 10.1016/j.bioelechem.2022.108135.

[97] A. Sabir *et al.*, "Surface-enhanced Raman spectroscopy for studying the interaction of N-propyl substituted imidazole compound with salmon sperm DNA," *Photodiagnosis Photodyn. Ther.*, vol. 41, p. 103262, Mar. 2023, doi: 10.1016/j.pdpdt.2022.103262.

[98] A. M. Oliveira-Brett, V. C. Diculescu, T. A. Enache, I. P. G. Fernandes, A.-M. Chiorcea-Paquim, and S. C. B. Oliveira, "Bioelectrochemistry for sensing amino acids, peptides, proteins and DNA interactions," *Curr. Opin. Electrochem.*, vol. 14, pp. 173–179, Apr. 2019, doi: 10.1016/j.coelec.2019.03.008.

[99] J. Wang *et al.*, "Interactions of antitumor drug daunomycin with DNA in solution and at the surface," *Bioelectrochemistry Bioenerg.*, vol. 45, no. 1, pp. 33–40, Mar. 1998, doi: 10.1016/S0302-4598(98)00075-0.

[100] H. Karimi-Maleh *et al.*, "Guanine-Based DNA Biosensor Amplified with Pt/SWCNTs Nanocomposite as Analytical Tool for Nanomolar Determination of Daunorubicin as an Anticancer Drug: A Docking/Experimental Investigation," *Ind. Eng. Chem. Res.*, vol. 60, no. 2, pp. 816–823, Jan. 2021, doi: 10.1021/acs.iecr.0c04698.

[101] S. Kurbanoglu, B. Dogan-Topal, L. Hlavata, J. Labuda, S. A. Ozkan, and B. Uslu, "Electrochemical investigation of an interaction of the antidepressant drug aripiprazole with original and damaged calf thymus dsDNA," *Electrochim. Acta*, vol. 169, pp. 233–240, Jul. 2015, doi: 10.1016/j.electacta.2015.04.087.

[102] P. Rebelo, J. G. Pacheco, M. N. D. S. Cordeiro, A. Melo, and C. Delerue-Matos, "Azithromycin electrochemical detection using a molecularly imprinted polymer prepared on a disposable screen-printed electrode," *Anal. Methods*, vol. 12, no. 11, pp. 1486–1494, 2020, doi: 10.1039/C9AY02566A.

[103] P. K. Singh *et al.*, "An exhaustive compilation on chemistry of triazolopyrimidine: A journey through decades," *Bioorg. Chem.*, vol. 88, p. 102919, Jul. 2019, doi: 10.1016/j.bioorg.2019.102919.

[104] H. Lan *et al.*, "Small-molecule inhibitors of FABP4/5 ameliorate dyslipidemia but not insulin resistance in mice with diet-induced obesity," *J. Lipid Res.*, vol. 52, no. 4, pp. 646–656, Apr. 2011, doi: 10.1194/jlr.M012757.

[105] N. V. Ortiz Zacarías *et al.*, "Synthesis and Pharmacological Evaluation of Triazolopyrimidinone Derivatives as Noncompetitive, Intracellular Antagonists for CC Chemokine Receptors 2 and 5," *J. Med. Chem.*, vol. 62, no. 24, pp. 11035–11053, Dec. 2019, doi: 10.1021/acs.jmedchem.9b00742.

[106] R. J. Moreau *et al.*, "Fragment-Based Drug Discovery of Inhibitors of Phosphopantetheine Adenylyltransferase from Gram-Negative Bacteria," *J. Med. Chem.*, vol. 61, no. 8, pp. 3309–3324, Apr. 2018, doi: 10.1021/acs.jmedchem.7b01691.

[107] G. S. Hassan, M. A. El-Sherbeny, M. B. El-Ashmawy, S. M. Bayomi, A. R. Maarouf, and F. A. Badria, "Synthesis and antitumor testing of certain new fused triazolopyrimidine and triazoloquinazoline derivatives," *Arab. J. Chem.*, vol. 10, pp. S1345–S1355, Feb. 2017, doi: 10.1016/j.arabjc.2013.04.002.

[108] H. Istanbullu, G. Bayraktar, I. Ozturk, G. Coban, and M. Saylam, "Design, Synthesis and Bioactivity Studies of Novel Triazolopyrimidinone Compounds," *J. Res. Pharm.*, vol. 26(1), no. 26(1), pp. 231–241, 2022, doi: 10.29228/jrp.121.

[109] F. Kurul, H. Istanbullu, H. O. Kaya, A. E. Cetin, and S. N. Topkaya, "Electrochemical Properties of Fused Pyrimidine-Triazole Heterocyclic Molecules as Novel Drug Candidates," *Turkish J. Pharm. Sci.*, vol. 0, no. 0, pp. 0–0, 2023, doi: 10.4274/tjps.galenos.2023.46095.

[110] J. Cha, T. Gilmor, P. Lane, and J. S. Ranweiler, "Stability Studies," 2011, pp. 459–505.

[111] E. Kanat, E. Eksin, B. Karacicek, Y. Eraç, and A. Erdem, "Electrochemical Detection of Interaction between Dacarbazine and Nucleic Acids in Comparison to Agarose Gel Electrophoresis," *Electroanalysis*, vol. 30, no. 7, pp. 1566–1574, Jul. 2018, doi: 10.1002/elan.201800064.

[112] D. E. Bayraktepe, "A voltammetric study on drug-DNA interactions: Kinetic and thermodynamic aspects of the relations between the anticancer agent dasatinib and ds-DNA using a pencil lead graphite electrode," *Microchem. J.*, vol. 157, p. 104946, Sep. 2020, doi: 10.1016/j.microc.2020.104946.

[113] S. Srinivas and A. Senthil Kumar, "Surface-Activated Pencil Graphite Electrode for Dopamine Sensor Applications: A Critical Review," *Biosensors*, vol. 13, no. 3, p. 353, Mar. 2023, doi: 10.3390/bios13030353.

[114] M. Buleandră, D. E. Popa, I. G. David, and A. A. Ciucu, "A simple and efficient cyclic square wave voltammetric method for simultaneous determination of epinephrine and norepinephrine using an activated pencil graphite electrode," *Microchem. J.*, vol. 160, p. 105621, Jan. 2021, doi: 10.1016/j.microc.2020.105621.

[115] P. Deng, Z. Xu, and Y. Kuang, "Electrochemically reduced graphene oxide modified acetylene black paste electrode for the sensitive determination of bisphenol A," *J. Electroanal. Chem.*, vol. 707, pp. 7–14, Oct. 2013, doi: 10.1016/j.jelechem.2013.08.020.

[116] P. Jakóbczyk, A. Dettlaff, G. Skowierzak, T. Ossowski, J. Ryl, and R. Bogdanowicz, "Enhanced stability of electrochemical performance of few-layer black phosphorus electrodes by noncovalent adsorption of 1,4-diamine-9,10-anthraquinone," *Electrochim. Acta*, vol. 416, p. 140290, Jun. 2022, doi: 10.1016/j.electacta.2022.140290.

[117] S. Bilge, B. Dogan-Topal, T. Taskin Tok, E. B. Atici, A. Sınağ, and S. A. Ozkan,

“Investigation of the interaction between anticancer drug ibrutinib and double-stranded DNA by electrochemical and molecular docking techniques,” *Microchem. J.*, vol. 180, p. 107622, Sep. 2022, doi: 10.1016/j.microc.2022.107622.

8. APPENDIX

8.1. NMR Spectra of Drug Candidate Molecules

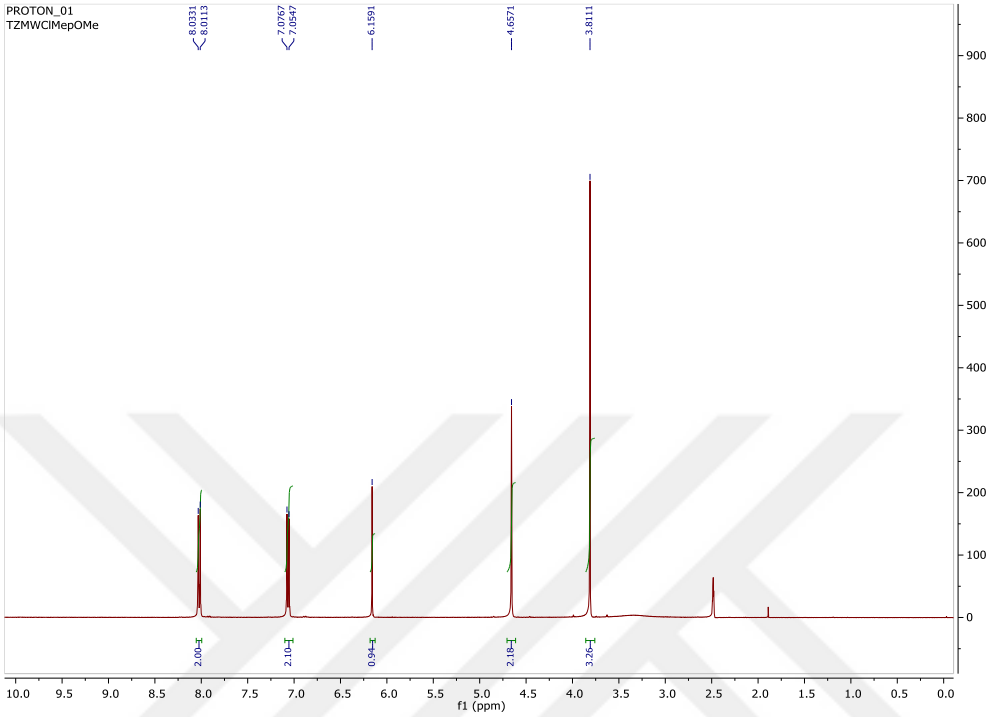


Figure S1. ^{1}H NMR Spectra of D_1-TP

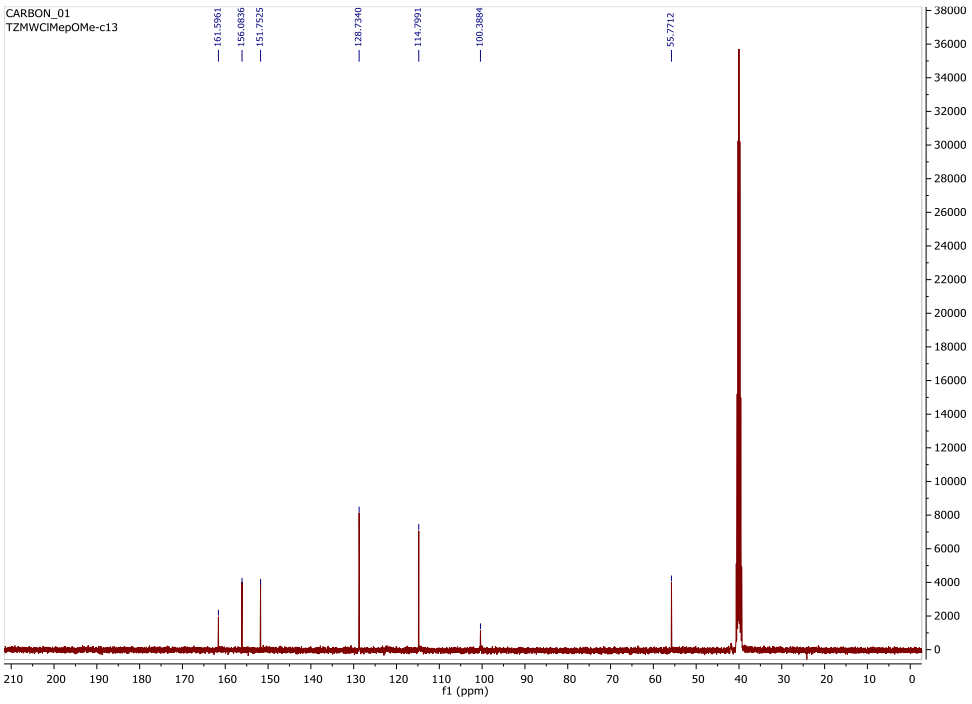


Figure S2. ^{13}C NMR Spectra of D_1-TP

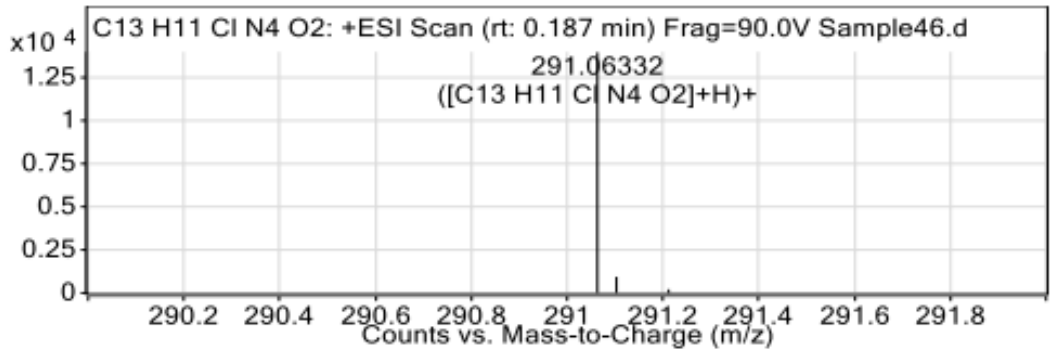
Qualitative Analysis Report

Data Filename	Sample46.d	**Sample Name**	Sample46
Sample Type	Sample	**Position**	P1-F1
Instrument Name	Instrument 1	**User Name**	Osman Nuri ASLAN
Acq Method	ESI pos.m	**Acquired Time**	9.03.2022 13:29:37
IRM Calibration Status	Success	**DA Method**	Default.m
Comment			

Sample Group		**Info.**	
Stream Name	LC 1	**Acquisition SW Version**	6200 series TOF/6500 series Q-TOF B.08.00 (B8058.0)

User Spectra

Fragmentor Voltage	Collision Energy	Ionization Mode
90	0	ESI



Peak List

m/z	z	Abund	Formula	Ion
291.06332	1	13984.74	C13 H11 Cl N4 O2	(M+H)+
313.04364	1	22951.55		
315.04157	1	6561.68		
329.01804	1	7036.92		
603.10071	1	101639.05		
604.10314	1	28659.66		
605.09877	1	67451.13		
606.09997	1	16867.94		
607.09646	1	11783.25		
619.07417	1	9988.45		

Formula Calculator Element Limits

Element	Min	Max
C	3	13
H	0	11
N	0	4
O	0	2
Cl	0	1

Formula Calculator Results

Formula	Best	Mass	Tgt Mass	Diff (ppm)	Ion Species	Score
C13 H11 Cl N4 O2	DOĞRU	290.05552	290.05705	5.29	C13 H12 Cl N4 O2	80.21

Figure S3. HRMS data of D_1-TP

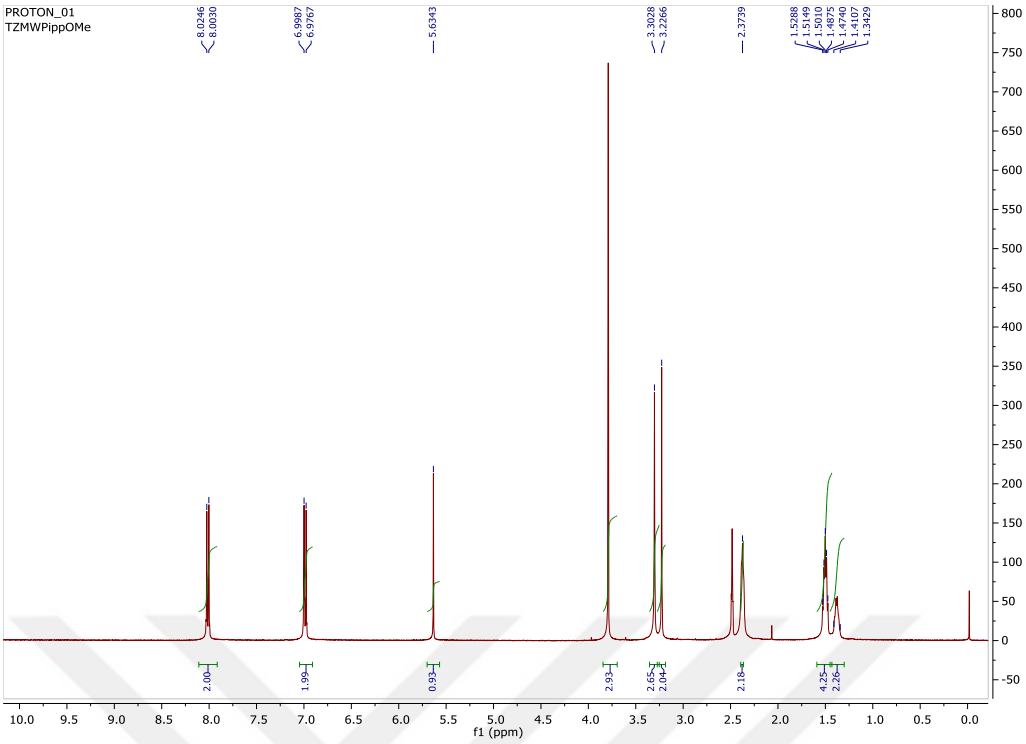


Figure S4. ^{1}H NMR Spectra of D_2-TP

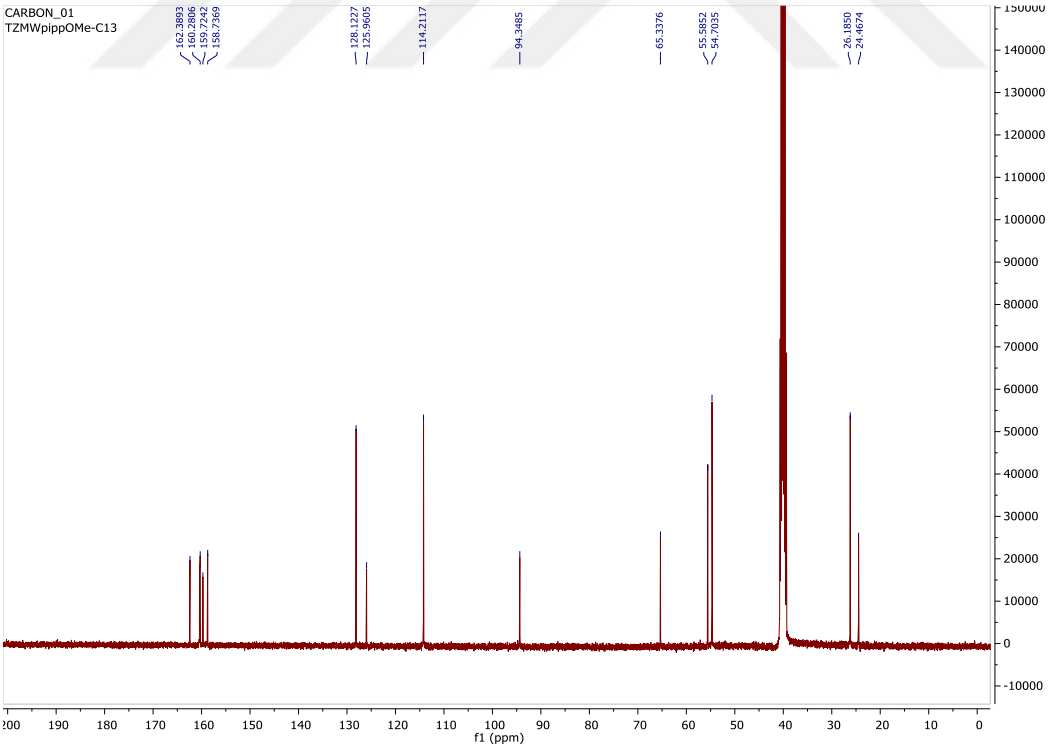


Figure S5. ^{13}C NMR Spectra of D_2-TP

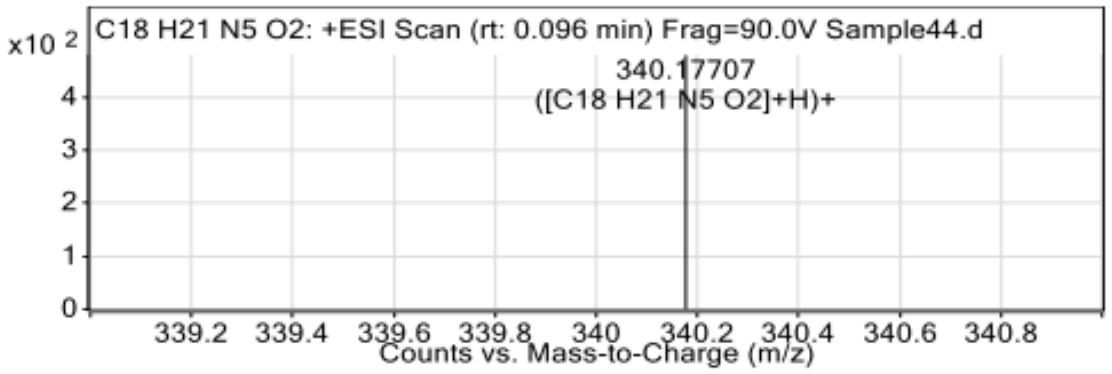
Qualitative Analysis Report

Data Filename	Sample44.d	**Sample Name**	Sample44
Sample Type	Sample	**Position**	P1-E8
Instrument Name	Instrument 1	**User Name**	Osman Nuri ASLAN
Acq Method	ESI pos.m	**Acquired Time**	9.03.2022 13:24:16
IRM Calibration Status	Success	**DA Method**	Default.m
Comment			

Sample Group		**Info.**	
Stream Name	LC 1	**Acquisition SW Version**	6200 series TOF/6500 series Q-TOF B.08.00 (B8058.0)

User Spectra

Fragmentor Voltage	Collision Energy	Ionization Mode
90	0	ESI



Peak List

m/z	z	Abund
100.01216		716
101.00172		758.46
102.12696		2935.24
125.98556		819.45
130.15831		1208.29
167.01174		868.47
185.11372	1	2942.39
362.15579	1	2343.85
378.1331		684.14
406.32531	1	1478.49

Formula Calculator Element Limits

Element	Min	Max
C	3	18
H	0	21
N	0	5
O	0	2

Formula Calculator Results

Formula	Best	Mass	Tgt Mass	Diff (ppm)	Ion Species	Score
C18 H21 N5 O2	DOGRU	339.16979	339.16952	-0.8	C18 H22 N5 O2	47.39

Figure S6. HRMS data of D_2-TP

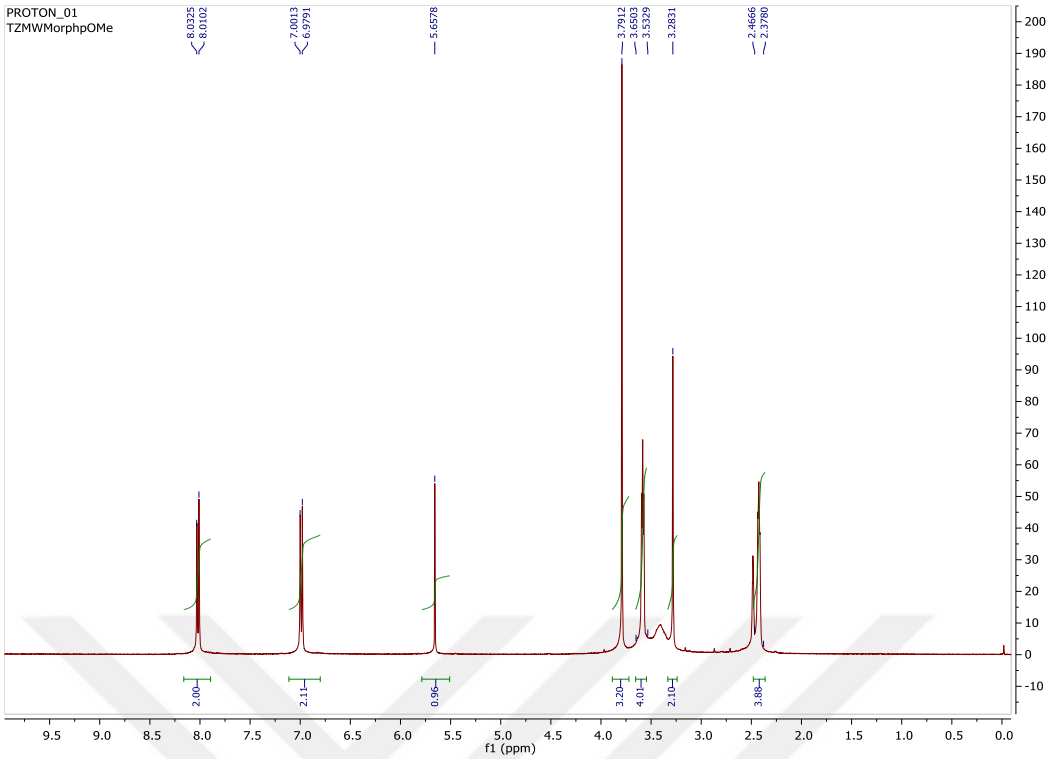


Figure S7. ^{1}H NMR Spectra of D_3-TP

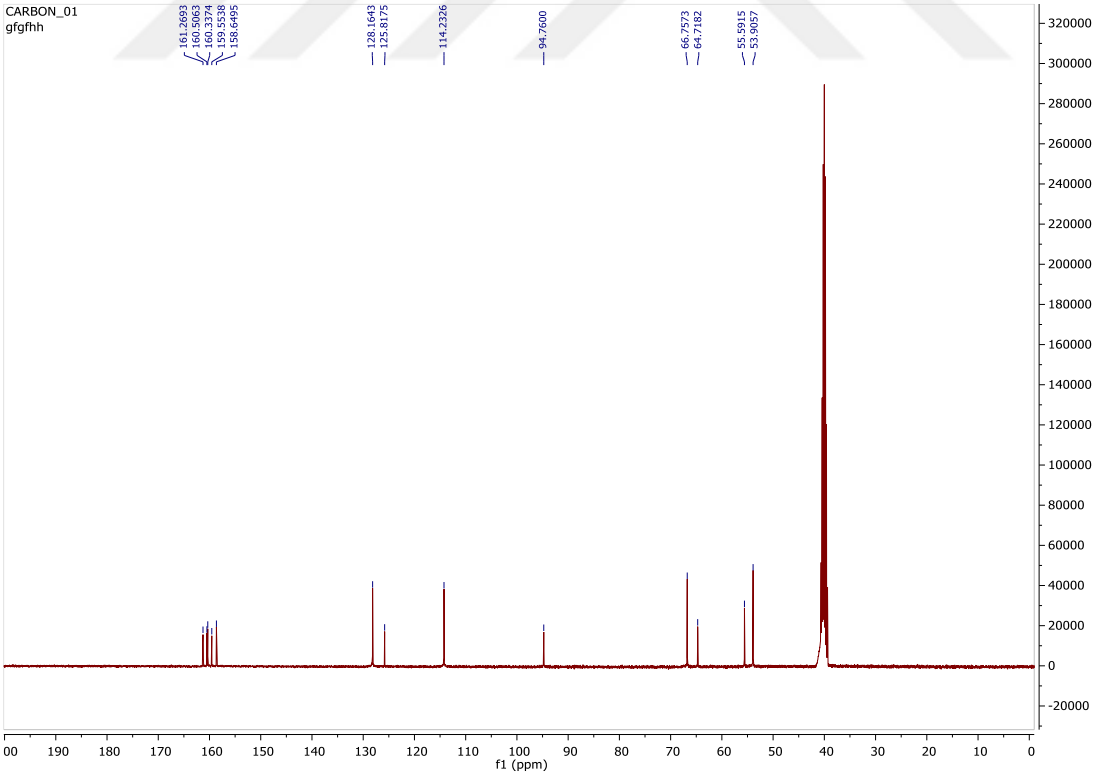


Figure S8. HRMS data of D_3-TP

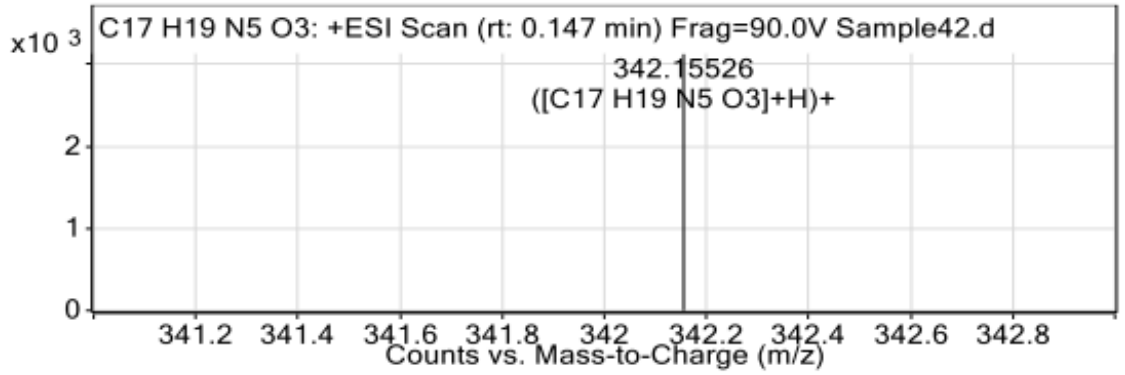
Qualitative Analysis Report

Data Filename	Sample42.d	**Sample Name**	Sample42
Sample Type	Sample	**Position**	P1-E6
Instrument Name	Instrument 1	**User Name**	Osman Nuri ASLAN
Acq Method	ESI pos.m	**Acquired Time**	9.03.2022 13:18:52
IRM Calibration Status	Success	**DA Method**	Default.m
Comment			

Sample Group		**Info.**	
Stream Name	LC 1	**Acquisition SW Versior**	6200 series TOF/6500 series Q-TOF B.08.00 (B8058.0)

User Spectra

Fragmentor Voltage	Collision Energy	Ionization Mode
90	0	ESI



Peak List

m/z	z	Abund	Formula	Ion
132.90359		4762.14		
210.91546		1435.13		
342.15526	1	3130.95	C17 H19 N5 O3	(M+H)+
474.05149	1	16621.97		
474.10335		1299.25		
475.05505	1	2978.97		
547.10823	1	1285		
605.94806	1	4872.07		
683.30168	1	1764.2		
815.19928	1	3132.83		

Formula Calculator Element Limits

Element	Min	Max
C	3	17
H	0	19
N	0	5
O	0	3

Formula Calculator Results

Formula	Best	Mass	Tgt Mass	Diff (ppm)	Ion Species	Score
C17 H19 N5 O3	DOĞRU	341.14814	341.14879	1.89	C17 H20 N5 O3	83.48

Figure S9. ^{13}C NMR Spectra of D_3-TP

8.2. Research Ethics Committee Approvals

İZMİR BİYOTIP VE GENOM MERKEZİ
GİRİŞİMSEL OLMAYAN ARAŞTIRMALAR ETİK KURULU (İBG-GOEK)
KARARI

Toplantı Tarihi	: 25/11/2021	**Toplantı Günü**	: Perşembe
Toplantı Sayısı	: 13	**Toplantı Saati**	: 10:30

Sayın Doçent Doktor Serhat TOZBURUN,

2021-041 Protokol No'lu; sorumlusu olduğunuz "Analitlerin Yüksek Hassasiyette Otomatik Nicel Analizine Yönelik Portatif Elektrokimyasal Biyosensör" başlıklı araştırmanın uygulanmasında etik açıdan sakınca olmadığına oy birliği ile karar verilmiştir.

Bilgilerinizi ve gereğini rica ederiz.

8.3. Curriculum Vitae

Name/Surname:	Fatma KURUL
Date of Birth:	01.01.1998
Place of Birth:	Burdur
E-posta	fatmakurul@outlook.com.tr

EDUCATION

University	Department	Degree	Graduation
Dokuz Eylul University/Izmir International Biomedicine and Genome Institute	Biomedicine and Health Technologies	Master`s Degree	2024
Pamukkale University Faculty of Technology	Biomedical Engineering	Bachelor Degree	2020

FIELD OF INTERESTS

Stem Cell Mechanobiology, Cell Culture, Intracellular Imaging Using Fluorescence Microscopy, Data Analysis, Nanotechnology, Biosensing, Electrochemical Biosensors, Microfluidic Systems

WORK EXPERIENCE

Position	Institution/Company
Visiting Research Student	Technical University of Munich, Munich, GERMANY
Intern Engineer	TUBITAK National Metrology Institute (UME), Kocaeli, TURKEY
Intern Engineer	Ertunc Ozcan Group of Companies, Ankara, TURKEY
Intern Engineer	Pamukkale University Hospital, Denizli, TURKEY

Intern Engineer	Pamukkale University, Biomedical Sciences Laboratory, Denizli, TURKEY

PUBLICATIONS

Sena Yaman, Meryem Beyza Avci, **Fatma Kurul**, Seda Nur Topkaya, Arif E Cetin, "Handheld Optofluidic Platform towards Binding Dynamics Applications in Field-Settings." ***Sensors and Actuators A: Physical***, pp.114685.

Fatma Kurul, Istanbullu Huseyin, Huseyin Oguzhan Kaya, Arif E. Cetin, Seda Nur Topkaya, "Electrochemical Properties of Fused Pyrimidine-Triazole Heterocyclic Molecules as Novel Drug Candidates", ***Turkish Journal of Pharmaceutical Sciences***, doi:10.4274/tjps.galenos.2023.46095, (2023).

Fatma Kurul, Ziya Ata Yazici, Zeynep A. Kocer, Seda Nur Topkaya, Arif E. Cetin. "Low-cost and portable plasmonic biosensor for label-free detection of viruses in resource-limited settings." ***In Translational Biophotonics: Diagnostics and Therapeutics III***, vol. 12627, pp. 241-247. SPIE, 2023.

Fatma Kurul, Hüseyin Istanbullu, Seda Nur Topkaya, "Electrochemical Profiling of a Promising Fused Pyrimidine-Triazole Drug Candidate", ***Erciyes University Journal of Institue of Science and Technology***, (2023).

Hüseyin Oğuzhan Kaya, Gokay Albayrak, Hasan Isbilir, **Fatma Kurul**, Sura Baykan, Yeni Wahyuni Hartati, Seda Nur Topkaya, "Electrochemical Profiling of Natural Furanocoumarins: DNA Interaction Dynamics of Oxypeucedanin and Prantschimgin", **ADMET & DMPK**, https://doi.org/10.5599/admet.2199 (2024).

(Under review) **Fatma Kurul**, Idil Karaca Acari, Meryem Beyza Avci, S. Deniz Yasar, Seda Nur Topkaya, Ceyhun Acari, Erbil Unsal, Balahan Makay, Suleyman Koytepe, Burhan Ates, Ismet Yılmaz, Turgay Seckin, Arif E. Cetin, "A Pre-Diagnostic Tool For a Rare Disease: Familial Mediterranean Fever (FMF)", ***Nature Communications***, (2023).

(Under review) Beyzanur Doruk, **Fatma Kurul**, Seda Nur Topkaya, "Green Chemistry and Its Applications, ***Turkey Clinics Health Sciences***", (2023).

(Submitted) **Fatma Kurul**, Hasret Turkmen, Arif E. Cetin, Seda Nur Topkaya, "Nanomaterials in Healthcare: Bridging the Gap with Nanomedicine", ***Journal of Drug Delivery Science and Technology***, (2023).

ORAL PRESENTATIONS

Fatma Kurul, Seda Nur Topkaya, Ozden Yalcin−Ozuysal, Ali Khademhosseini, Arif E. Cetin, "Advancing Single Cell Growth Measurement: A Plasmonic Functional Assay Platform with Refractive Index Sensing", ***33rd International Symposium on Pharmaceutical and Biomedical Analysis (PBA 2023)***, July 2023, Ankara, TURKEY.

POSTER PRESENTATIONS

Fatma Kurul, Damla Aydogan, Ziya Ata Yazici, Zeynep A. Kocer, Seda Nur Topkaya, Arif E. Cetin, "Cost-effective Plasmonic Biosensor Platform for Label-free Virus Detection", ***International Multidisciplinary Symposium on Drug Research and Development (DRD) 2023***, May 2023, Izmir, TURKEY.

Fatma Kurul, Ziya Ata Yazici, Zeynep A. Kocer, Seda Nur Topkaya, Arif E. Cetin, "Low-Cost and Portable Plasmonic Biosensor for Label-Free Detection of Viruses in Resource-Limited Settings", ***SPIE-OPTICA The European Conferences on Biomedical Optics/Translational Biophotonics: Diagnostics and Therapeutics***, June 2023, Munchen, GERMANY.

Fatma Kurul, Ziya Ata Yazici, Seda Nur Topkaya, Ozden Yalcin-Ozuysal, Arif E. Cetin, "Exploring Cancer Cell Therapeutic Profiles with the Plasmonic Functional Assay Platform", ***National Optical, Electro-Optical, and Photonics Workshop***, Sep 2023, İstanbul, TURKEY.

Ceylin Bozdemir, **Fatma Kurul**, Hüseyin İstanbullu, Seda Nur TOPKAYA, "Evaluation of the Electrochemical Characteristics of Triazolopyrimidinone Derivatives as Novel Drugs and Determination of Their Interactions with DNA" ***33rd International Symposium on Pharmaceutical and Biomedical Analysis (PBA 2023)***, July 2023, Ankara, TURKEY.

ACHIEVEMENTS, HONOURS & AWARDS

-Being among the final six projects in the initiative supporting famous women entrepreneurs from UNLU & CO (2023)

-Came in second in Future of Laboratories^2 Incubation Program (2023)

-Received research grant from TUBITAK 2224-A International Scientific Meetings Fellowship Programme (2023)

-Received a scholarship from the Erasmus+ Traineeship Mobility program for a summer internship at the Technical University of Munich, Nano and Microrobotics Laboratory (2022)

-Received the Best Presentation Award in the Artificial Intelligence in Health Competition in TEKNOFEST (2022)

-Received the Achievement Plaque from Bursa Technical University (2022)

-Received the Jury Special Award in the Artificial Intelligence in Health Competition in TEKNOFEST (2022)

-Came in second in the Biotechnology Innovation Category in TEKNOFEST (2021)

-Received the bronze medal at TEKNOFEST (2021)

-Received research grant from TUBITAK 2210/D National Industrial MSc Scholarship Program (2021)

-Graduated as a High Honour Student (2020)

-Graduated with a Top Student in the Department (2020)

CERTIFICATES

-Innovative Entrepreneurship Training-KOSGEB

-Feb 2021, Polymerase Chain Reaction (PCR) Method and Real-Time PCR Webinar-Lab Academy

-Jan 2021, Laboratory Safety and Working Rules-Lab Academy

-Jan 2021, BioTech Artificial Tissues-Beykent University

-Jan 2021, Entrepreneur-Entrepreneurship Society of IZTECH

-Nov 2020, 8th National Bioengineering Student Congress-IZTECH

-Oct 2019, General Metrology Seminar- TUBITAK National Metrology Institute

CLUB & ASSOCIATION MEMBERSHIPS

2023-Present, Society of Photo-Optical Instrumentation Engineers (SPIE) Member

2020-Present Turkey Technology Team Foundation

2020-2021, IEEE IZTECH Student Branch

2019-2020, Gebze Technical University Bioengineering Society (GTU BIOS)